

RESEARCH ARTICLE

Transcriptomics analysis of *in vivo* *Opisthorchis viverrini*: Stage-specific gene expression and novel genes with stable expression in mammalian stages for opisthorchiasis intervention

Waraporn Taweesin¹, Siriyakorn Kulwong², Wassana Jamnongkan³, Wichit Taron³, Autchaisai Siriprayong⁴, Sirinya Sitthirak^{2,5}, Anchalee Techasen⁴, Opal Pitaksakulrat⁶, Nisana Namwat^{2,3}, Poramate Klanrit^{2,3}, Watcharin Loilome^{2,3}, Arporn Wangwiwatsin^{2,3*}



1 Department of Biochemistry, Faculty of Medicine, Khon Kaen University, Khon Kaen, Thailand, **2** Department of Systems Biosciences and Computational Medicine, Faculty of Medicine, Khon Kaen University, Khon Kaen, Thailand, **3** Cholangiocarcinoma Research Institute, Khon Kaen University, Khon Kaen, Thailand, **4** Department of Medical Technology, Faculty of Associated Medical Sciences, Khon Kaen University, Khon Kaen, Thailand, **5** School of Allied Health Sciences, Walailak University, Nakhon Si Thammarat, Thailand, **6** Department of Parasitology, Faculty of Medicine, Khon Kaen University, Khon Kaen, Thailand

* arpowa@kku.ac.th

OPEN ACCESS

Citation: Taweesin W, Kulwong S, Jamnongkan W, Taron W, Siriprayong A, Sitthirak S, et al. (2025) Transcriptomics analysis of *in vivo* *Opisthorchis viverrini*: Stage-specific gene expression and novel genes with stable expression in mammalian stages for opisthorchiasis intervention. PLoS Negl Trop Dis 19(12): e0013714. <https://doi.org/10.1371/journal.pntd.0013714>

Editor: Eduardo José Lopes-Torres, Rio de Janeiro State University: Universidade do Estado do Rio de Janeiro, BRAZIL

Received: December 31, 2024

Accepted: November 3, 2025

Published: December 18, 2025

Copyright: © 2025 Taweesin et al. This is an open access article distributed under the terms of the [Creative Commons Attribution License](#), which permits unrestricted use, distribution, and reproduction in any medium, provided the original author and source are credited.

Data availability statement: The raw data were publicly deposited at ENA under accession number ERP150740.

Abstract

Opisthorchis viverrini, Southeast Asian liver fluke, is a parasitic flatworm that has been widely spread in Asia and is a major risk factor for bile duct cancer - cholangiocarcinoma (CCA). Over 12 million people are at risk of opisthorchiasis, and the associated CCA is known to have claimed around 20,000 deaths per year in Thailand alone, with the number projected to be underestimated elsewhere. There is an opportunity to develop more efficient drug targets and diagnostic biomarkers, and these are urgently needed. Despite previous studies on gene expression analysis and reference genome, the knowledge on the biological processes of *O. viverrini* during its development remains largely unclear. Our study employed RNA-sequencing transcriptomics of *O. viverrini* developmental stages within hamsters from the juvenile stage (14-day post-infection), the adult stage of acute infection (42 days), and the adult stage of chronic infection (180 days). Differential gene expression and functional analyses were performed, and genes with stable expression (GSEs) were identified based on the transcript per million (TPM) normalization method and coefficient of variation. Our results show that key genes in juveniles were mostly associated with proteolysis, energy metabolism, signal transduction, and development. Significantly up-regulated genes in adult *O. viverrini* were associated with parasitic reproductive systems and parasitism. A total of 2,011 GSEs were identified, with 27 genes being highly expressed, and 628 genes showing no orthologues in the human reference genome. From this novel dataset, we illustrated insight into parasite biology, which

Funding: This research was supported by the National Science Research and Innovation Fund (NSRF) and the Research Program from Research Department of Khon Kaen University under the Basic Research Fund of Khon Kaen University through Cholangiocarcinoma Research Institute to AW. WaT is sponsored through studentship from the Institute for the Promotion of Teaching Science and Technology. The sponsors or funders do not play any role in the study design, data collection and analysis, decision to publish, or preparation of the manuscript.

Competing interests: The authors have declared that no competing interests exist.

revealed key molecular processes during intra-mammalian infection, and provided the candidate targets for biomarkers, drugs, and vaccine development. This valuable information will contribute to opisthorchiasis diagnostics and prevention in endemic countries and provide leads for future characterization of essential genes across liver fluke species.

Author summary

Opisthorchis viverrini, a liver fluke parasite, infects millions of people in Southeast Asia and is a leading cause of bile duct cancer, a disease with high fatality rates. People become infected by eating raw or undercooked freshwater fish carrying the parasite. Chronic infections often go unnoticed but can cause severe liver damage and inflammation, increasing the risk of cancer over time. Current diagnostic methods have improved, but still face challenges, such as false positives caused by similar parasites. Better tools for diagnosing and understanding this parasite are urgently needed to reduce its impact on public health. In this study, we examined how the parasite's genes are turned on and off during its life stages inside a mammalian host. By analyzing parasites from an established hamster model, we identified genes that are active in the parasite during early infection, adulthood, and long-term chronic infection. We also discovered over 2,000 genes that the parasite used during infection in a mammalian host. These genes include some that are not found in humans and might be promising specific targets for intervention. Our findings provide a roadmap for developing more precise diagnostic tools and potential therapies, helping to combat this neglected tropical disease and its deadly complications.

Introduction

Opisthorchis viverrini is a food-borne parasitic flatworm (liver fluke) that causes an infection known as opisthorchiasis. Opisthorchiasis has been widely spread in countries around the Great Mekong Subregion river, including Thailand, Laos, Cambodia, and Vietnam, and is a major risk factor for bile duct cancer, or cholangiocarcinoma (CCA) [1]. To develop their life cycles, *O. viverrini* typically reside in three major diverse hosts for the different developmental stages, which include snails (the first intermediate hosts for the cercariae stage), fishes (the second intermediate hosts for the metacercarial stage), and humans that acts as the last infective hosts for adult worms. Following the infection to human contracted by consuming raw infective freshwater fish, or salted preserved fish contaminated with *O. viverrini* metacercaria, left untreated, chronic liver fluke infection can eventually lead to CCA development driven by many infection-associated factors including the roles of liver fluke's excretory/secretory (ES) products, proteases, and inflammation-induced DNA damage. [2,3]. Recent published statistics of opisthorchiasis and CCA prevalence during 2013–2019

showed that over 85,323 (32.37% of total 263,588 participants) people are at risk of opisthorchiasis, and the associated CCA is diagnosed at 948 individuals (0.36% of all participants) [4], and claiming around 39–61 deaths per 100,000 in 2005 in Thailand alone [5]. Furthermore, the traditional ingestion of raw freshwater fish infected with *O. viverrini* is a major factor attributing to opisthorchiasis, which account for approximately 12 million people in Thailand, Laos, Cambodia, and Vietnam [6]. This high infection is strongly associated with CCA, causing approximately 20,000 deaths annually [1].

Current interventions involve routine urine- or stool-based diagnosis and treatment with praziquantel (PZQ). Although PZQ treatment is effective, only the adult stage responds effectively to PZQ [7], and re-infection can increase the risk of CCA development [8]. Nowadays, molecular-based detection of *O. viverrini* antigens using urinary samples is more comfortable and more rapid than fecal egg count examinations. What is more, the molecular-based method has demonstrated higher sensitivity, specificity, and consistency for the diagnostic and screening of *O. viverrini* infection [9,10]. However, the latest antigen-based detection still has some cross-species reactions [11]. Therefore, a comprehensive understanding of parasite biology is necessary for developing effective and suitable diagnosis and disease intervention strategies, including new target drugs or vaccine discovery, candidate biomarkers for opisthorchiasis diagnosis, and prevention of helminth infection.

Omics has been a valuable technique to study various biomolecular processes and comprehend the complex relationships among DNAs, RNAs, proteins, and metabolites by the integration of multiple omics [12]. Particularly, transcriptomics through RNA-seq analysis enables the profiling of all transcripts and their underlying molecular mechanisms, providing valuable insights into how gene expression is modulated in response to pathological conditions within cells or organisms [13–15]. Previous transcriptomic work allows us to understand some molecular mechanisms of *O. viverrini* from juvenile (14 days post-infection) to adult (42 days infection). However, the study's scope was limited in its exploration of host-parasite interactions, and life stage-specific data, but lacked worms from the chronic infection stage, and no clear description of biological replicates [16]. Since the first genome of *O. viverrini* was successfully characterized and provided the insight into parasite biology as well as the association of CCA and *O. viverrini* [17], the gene information derived by this genome were applied for serving more in-depth research goals; for instance, to understand the effects of gene expression from *O. viverrini* in diabetic hamsters for opisthorchiasis control in diabetic patients [18]. Furthermore, based on this reference genome, several studies were able to investigate molecular mechanisms through specific proteins in *O. viverrini*; for instance, the role of serpins and cystatins in fibrinolysis and cysteine proteinase activity has been explored [19,20]. Nevertheless, the comprehensive molecular mechanism expressed by *O. viverrini*, investigated via the lens of a comprehensive transcriptomics study, remains lacking.

To fill these knowledge gaps, and enlist novel candidate biomarkers as well as potential drug targets, we conducted RNA-seq analysis to identify differentially expressed genes in mammalian stages during a developmental timecourse from the hamster model, encompassing *ex vivo* *O. viverrini* 14-days, 42-days, and 180-days post-infection. Moreover, for the first time, we have revealed the list of *O. viverrini* housekeeping genes during the mammalian stage as well as proposing stage-specific candidate genes for the further characterization and development of drug and vaccine targets, key biomarkers for opisthorchiasis prevention and diagnosis.

Methods

Ethics statement

All animal procedures were conducted according to protocols approved by the Institutional Animal Care and Use Committee of Khon Kaen University, based on the Ethical Principles and Guidelines For The Procedures on Animals for Scientific Purposes of the National Research Council of Thailand, with the project license number IACUC-KKU-25/65.

Host infection and *O. viverrini* collection

The collection of *O. viverrini* metacercaria from cyprinoid fish was performed using pepsin digestion [21]. In brief, the fish were finely cut using a household blender machine for 3–5 minutes. The semi-fluid mass was then further digested using

a mixture of 0.25% pepsin (Wako Pure Chemical Industries, Osaka, Japan) and 1.50% HCl (RCI Labscan) in 0.85% NaCl solution, incubated at 37–40 °C in a water bath for one and a half hours with regular stirring. After the incubation, the mixture was filtered through 800, 300, 106, and 250 µm wire mesh sieves, respectively. The final pass-through, which contained metacercaria, was left to precipitate for 5–10 minutes in a beaker or until the supernatant became clear, then the supernatant was removed. Half of the beaker containing the metacercaria was filled with 0.85% NaCl solution to wash out the residual pepsin and HCl, and left for 5–10 minutes for the metacercaria to precipitate. Finally, the metacercaria was transferred to a Petri dish under a stereo microscope for further separation of the parasite from other fish debris.

The *O. viverrini* metacercaria were used for the infection in hamsters within 24 hours of isolation. Golden Syrian hamsters, MDKKU strain, were divided into three groups according to timepoints of 14 days, 42 days, and 180 days parasite collection post-infection, which reflected the early, acute, and chronic *O. viverrini* infection within the mammalian host. The D14 and D42 conditions might reflect important transcriptome changes in juvenile and acute adult stages [16] while the 6-month samples reflect chronic stages linked to host immune suppression, liver pathogenesis, and ultimately led to CCA development in the mammalian host [22,23]. The individual hamster was infected with 50 metacercaria using 25 ga intragastric tube via oral gavage. The hamsters were maintained at the Animal House Facility, Faculty of Medicine, Khon Kaen University, Thailand. At each timepoint of sample collection, the hamsters were euthanized with an overdose of isoflurane (Sigma Aldrich). *O. viverrini* was recovered from the bile duct of infected hamsters at different timepoints by gently squeezing the liver and observing under a stereo microscope. To preserve the *O. viverrini* for transcriptomes, the worms were washed in normal saline (Sigma Aldrich), and the pool of worms from each hamster, considered one replicate, were stored in 1 ml of TRIzol (Invitrogen) at -80 °C until RNA extraction. Overall workflow of this study is illustrated in Fig 1.

RNA extraction

Total RNAs of worms from each condition were extracted following the standard TRIzol-chloroform method, followed by RNA Clean & Concentrator-5 kit (Zymo Research). Briefly, the parasite samples stored in -80 °C were thawed on ice; samples were gently pipetted to mix and transferred to a new 2 ml MagNa tube containing ceramic beads (Roche). Homogenization

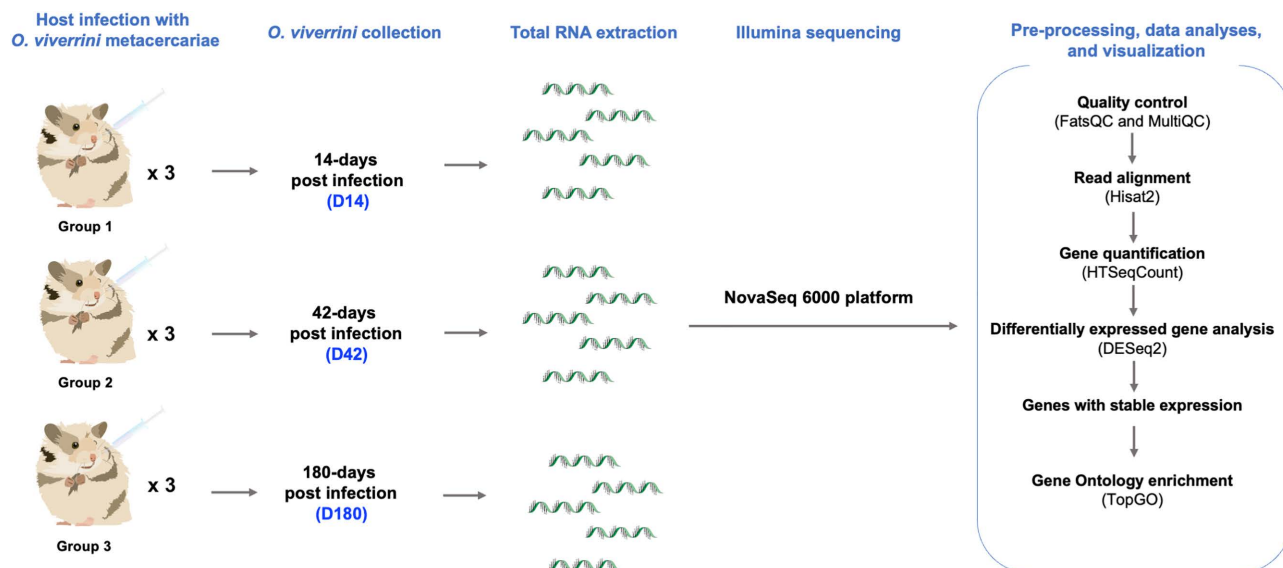


Fig 1. Study design of *O. viverrini* transcriptomics. Golden Syrian hamsters were used as hosts for *O. viverrini* infection. Parasites were collected at three timepoints post-infection for total RNA extraction and mRNA sequencing. RNA-seq data were analyzed using established bioinformatic tools.

<https://doi.org/10.1371/journal.pntd.0013714.g001>

by bead-beating machine was performed at maximum speed for 20 seconds, rested on ice for 1 minute, and then another 20 seconds at maximum speed. Then, the samples were transferred back to a LoBind microfuge tube (Eppendorf). In phase preparation step, 200 μ L chloroform was added per 1 mL of TRIzol reagent, and the sample was mixed vigorously by shaking for 5 seconds, incubated at room temperature for 2–3 minutes, and centrifuged at 12,000xg at 4 °C for 15 minutes. To collect the RNA, the upper aqueous phase was transferred by gentle pipetting to a new LoBind microfuge tube, an equal volume of 100% ethanol (RCI Labscan Group) was added, and the mixture was mixed well by pipetting. The mixture was immediately transferred to a Zymo-Spin column, centrifuged and washed according to the Zymo Clean & Concentrator protocol, and eventually eluted with 20 μ L DNase/RNase-free water. The extracted RNA was quantified using a NanoDrop spectrophotometer, and its integrity was evaluated using agarose gel electrophoresis and 4150 Agilent TapeStation.

RNA-sequencing

The extracted total RNAs under all of 3 conditions, including 14-days (D14), 42-days (D42), and 180-days (D180) post-infection, were sent to a Biomarker Technologies (BMKGENE) company in Beijing, China for mRNA sequencing with 150 bp read length, paired-end PE150 using the Illumina NovaSeq 6000 platform to obtain approximately 6 GB of data per sample. Subsequently, the obtained RNA-seq outputs were used for data analyses, and the raw data have been deposited at ENA under accession number ERP150740.

Pre-processing of RNA-seq data

The RNA-seq data at three timepoints in FASTQ file formats were used to perform quality control (QC) with FastQC [24] and MultiQC tools [25], using Phred score of > 30. For read mapping, the RNA-seq data were aligned to the indexed reference genome of *O. viverrini* obtained from WormBase Parasite, version WBPS19 [17], using Hisat2 (version 2.2.1) [26]. The resulting Sequence Alignment Map (SAM) file was subsequently converted into a Binary Alignment Map (BAM) format using SAMtools (version 1.12) [27]. Gene counts were quantified using HTSeq-count (version 1.99.2) [28] against the reference Genetic Feature Format version 3 (GFF3) annotation of *O. viverrini* obtained from WormBase Parasite version WBPS19 with default parameters, and mapped to coding sequence regions (CDS). Read count tables for all samples ([S1 File](#)) were then imported into the R program (version 4.2.3) [29].

Differential expression analysis

The DESeq2 package (version 1.38.3) [30] was used for pairwise comparisons between D14 versus D42, D14 versus D180, and D42 versus D180. All CDS counts files were used to generate metadata, which included information about sample name, file name, conditions (D14, D42, and D180), and their replicates. The DESeq2 objects were then created through an HTSeq counts matrix, normalized, and transformed into the rlog value using the DESeq2 package. The r-log-transformed values were used to perform multivariate analysis, represented by principal component analysis (PCA). The analysis of DEG was performed with the Wald test statistics with absolute \log_2 fold change (log2FC) greater than 1, and the adjusted p-value less than 0.01 as a cut-off for calling significantly up- and down-regulated genes. DEG results were displayed using ggplot2 package (version 3.4.4) [31] and R program (version 4.2.3).

Genes with Stable Expression of *O. viverrini* (GSEs)

To identify the GSE of *O. viverrini*, the non-normalized CDS counts stored in DESeq2 objects were derived from every condition and replicates for TPM normalization following the formula (1) [32]. The information on gene length in kilobases (Kb), the gene or exon length of *O. viverrini*, was retrieved from BioMart on WormBase Parasite version WBPS19 [33].

$$\text{Transcript per million or TPM} = \frac{\text{Non-normalised CDS count} / \text{gene length}}{\text{Sum (non-normalised count} / \text{gene length)}} \times 10^6 \quad (1)$$

All TPM-normalized data were used for gene expression variation measured in coefficient of variation (CV), as displayed in formula (2). If a gene has a CV value that is less than or equal to 0.15, the gene is assigned as GSE [34,35].

$$\text{Coefficient of variation or CV} = \frac{\text{Standard deviation of TPM}}{\text{Mean of TPM}} \quad (2)$$

Bioinformatic investigation of *O. viverrini* genes

All interesting genes of *O. viverrini* were searched on databases and publicly available bioinformatic tools to confirm both orthologues and non-orthologues to other species, as well as the similarity of protein sequence. To validate the non-human orthologues in *O. viverrini*, the interesting gene ID list was searched on WormBase Parasite version WBPS19 BioMart [33]. Selected outputs of interest were exported as *O. viverrini* gene ID, gene description, human orthologues ID, human orthologues name, % identity, etc. To confirm orthologues to another species, the gene ID list was used with a similar pipeline with a specific species name. Furthermore, gene sequences were further investigated using Basic Local Alignment Search tool (BLAST) [36]

Gene Ontology (GO) enrichment analysis

The GO enrichment was performed to assess functional analysis of both DEGs and GSEs using the topGO package (version 2.50.0) [37]. The GO term reference of the *O. viverrini* was acquired via BioMart on WormBase Parasite. The workflow of data pre-processing, DEG analysis, and GO term enrichment analysis followed a pipeline similar to those conducted in previously published studies [38–40].

Results

General statistics of RNA-seq data

The RNA-seq was performed on *O. viverrini* samples collected at 14, 42, and 180 days post-infection from experimentally infected Golden Syrian hamsters (Table 1). The sequencing platform generated an average of ~30 gigabase (Gb) for all nine samples, resulting in 19–23 million reads per sample. The RNA-seq quality control results using FASTQC demonstrated the good quality in base calling, with quality scores exceeding 30 in all samples. The GC content was 47%, which is consistent with that of the *O. viverrini* coding sequences previously published [16,17]. Furthermore, approximately ninety percent of the generated RNA-seq reads were successfully mapped to the current reference genome of *O. viverrini* (Table 1), indicating a clean sample collection.

Table 1. Sequencing output parameters of *O. viverrini* RNA-seq data.

Condition	The number of worms collected from each hamster	Sample name	% GC content	Total sequenced reads	Percentage of reads mapped to <i>O. viverrini</i> reference genome
D14	19	Ov_reads_1_1.sam	47	22,292,275	92.15
D14	17	Ov_reads_1_2.sam	47	21,185,106	91.62
D14	13	Ov_reads_1_3.sam	47	21,878,175	90.02
D42	37	Ov_reads_2_1.sam	47	21,093,539	83.30
D42	31	Ov_reads_2_2.sam	47	21,855,661	91.53
D42	31	Ov_reads_2_3.sam	47	19,168,246	91.19
D180	26	Ov_reads_3_1.sam	47	21,591,435	92.32
D180	27	Ov_reads_3_2.sam	47	21,024,778	92.44
D180	25	Ov_reads_3_3.sam	47	23,377,363	92.38
% Average reads mapped to genome					90.77

<https://doi.org/10.1371/journal.pntd.0013714.t001>

Transcriptomics profiles of *O. viverrini* during intramammalian infection

To comprehensively investigate the parasite biology of *O. viverrini* over developmental stages in a mammalian host, we performed principal component analysis (PCA) on the rlog-transformed gene read count using DESeq2 [30]. Consistent with our expectations, the PCA revealed most RNA-seq data captured by the first principal component (PC1), with 94% of total variance in the data on the PC1 axis. Conversely, the second principal component (PC2) explained only 2% of the variance (Fig 2). The PCA analysis indicates that the gene expression profiles were distinctly different between the juvenile (D14) and adults (D42 and D180). The two adult groups exhibited a complementary transcriptome profile demonstrated by their close proximity clustering; yet the replicates within each group suggested that there were some inter-group differences.

Numerous differentially expressed genes were identified when gene expression between juvenile and adult stages was compared. At D14, the juvenile worms up-regulated 524 genes in comparison to D42, whereas the D42 worms up-regulated 1,255 genes (Fig 3 and S1 Table). In a pairwise comparison between D14 and D180, 905 and 1,744 up-regulated genes in D14 and D180, respectively (Fig 3 and S2 Table). Finally, between the adult worms from acute and chronic phases of infection, D42 versus D180, only a small number of differentially expressed genes were identified; five genes were up-regulated in D42 worms and another five genes were up-regulated in D180 worms (Fig 3 and S3 Table).

Amongst the differentially expressed genes, there were lots of known genes that may play key roles in the fundamental biological functions of parasitic worms within mammalian hosts. In order to comprehensively describe the infection biology of *O. viverrini*, we investigated at each timepoint the top up-regulated genes that may directly influence their biology.

As displayed in Table 2, multiple genes associated with the biological process of the breakdown of proteins or peptides into smaller amino acids were up-regulated in D14 compared to D42 *O. viverrini*. All these genes represent log2FC between 3.08 and 7.89 (approximately 8–237 fold higher expression in D14), such as *peptidase A1 domain-containing protein* (T265_11050, T265_11760, and T265_13674), *peptidase C13 family protein* (T265_09482, T265_11933), and *legumain* (T265_10755, T265_12094, T265_15375, and T265_15407)

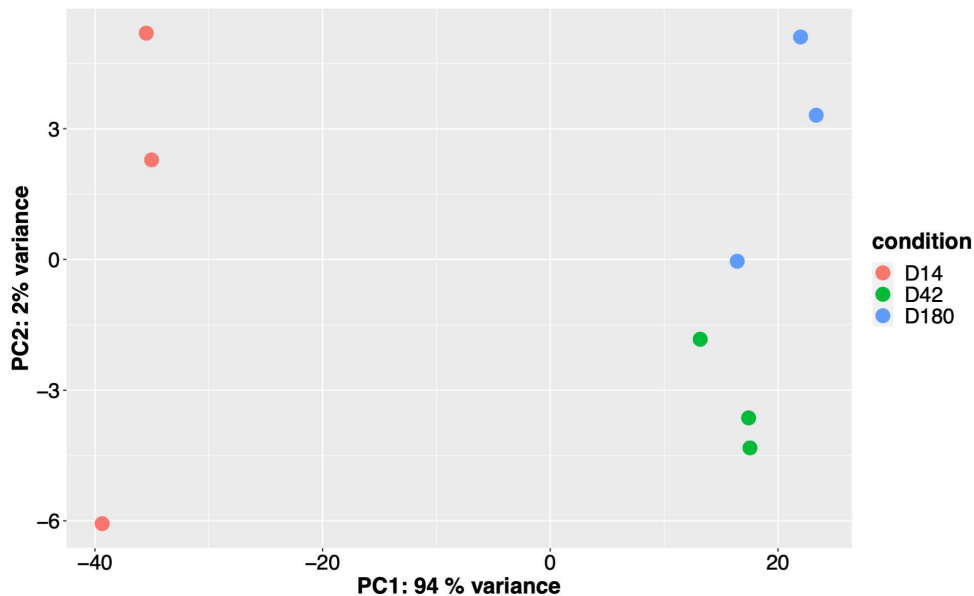


Fig 2. Principal component analysis of the *O. viverrini* RNA-seq data. The PCA plot showed the RNA-seq data clustering based on gene expression profiles using rlog-transformed values derived from DESeq2-normalized counts. Each data point represents a biological replicate, a pool of worms collected from one hamster host, and the color indicated the timepoints of sample collection.

<https://doi.org/10.1371/journal.pntd.0013714.g002>

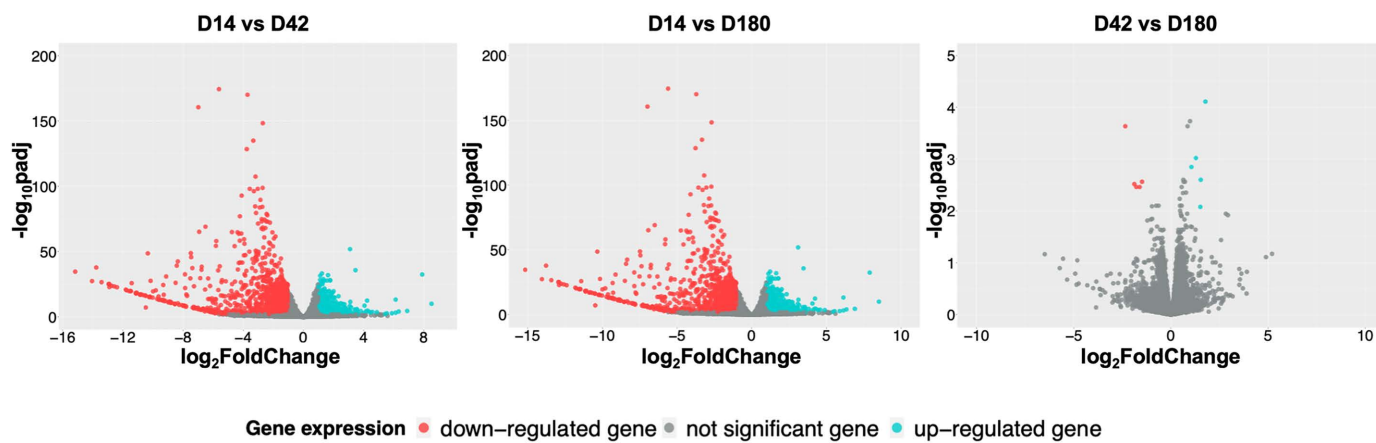


Fig 3. Pairwise comparisons between all timepoints. Volcano plots of pairwise comparisons of differential gene expressions of D14 vs D42 (juvenile worms compared to adult worms from acute infection stage), D14 vs D180 (juvenile worms compared to adult worms from chronic infection stage), and D42 vs D180 (adult worms from acute stage compared to those from chronic infection stage). The light blue dots indicate up-regulated genes with $\log_2\text{FC} > 1$ and adjusted p-value < 0.01 . The red dots were the down-regulated genes with $\log_2\text{FC} < -1$ and adjusted p-value < 0.01 . Genes that failed either $\log_2\text{FC}$ or adjusted p-value cut-offs were indicated in grey. Detailed results of all pairwise comparison is available in [S1–S3 Tables](#).

<https://doi.org/10.1371/journal.pntd.0013714.g003>

Functional analysis using GO enrichment supported that the up-regulated genes of juvenile (D14) *O. viverrini* were enriched in the proteolysis process. With 37 up-regulated genes annotated with the GO term, examples of these are *metalloendopeptidase*, *peptidase M12B*, *peptidase family M13*, *Peptidase C13 family*, *trypsin*, *legumains*, *peptidase A*, *peptidase A1*, *peptidase S1*, *peptidase_M14* (Fig 4 and S4 Table). These findings further corroborate the notion that a diverse peptidase gene, in addition to promoting energy utilization, may also contribute to their successful host invasion and immune modulation within hostile environment of the host's bile duct [41–44]. In line with this, the neuropeptide signaling pathway was also enriched among the D14 up-regulated genes, including three genes related to G-protein coupled receptors (T265_00683, T265_00777, T265_06423) and a putative neuroendocrine protein with proteolytic function (T265_14272) (Fig 4 and S4 Table).

During the juvenile stage, several genes known to be related to development and cell differentiation, which require strict signaling regulation, were highly expressed. These include genes encoding *Homeobox (Hox) domain-containing protein* (T265_04509), *PI3K/PI4K domain-containing protein* (T265_14809), and *TGF- β domain-containing protein* (T265_13153 and T265_05750). Other genes representing various points in signaling cascades were also up-regulated in D14 including *guanylate cyclase* (T265_12947), *Protein tyrosine phosphatase* (T265_12471, T265_12698), *Ras family protein* (T265_10821, T265_15294), *Ras-like protein family member 10B* (T265_09665), *Ras-like GTP-binding protein Rho1* (T265_09132), *Phosphoinositide interaction domain (PID) domain-containing protein* (T265_15658), and *cAMP-dependent protein kinase* (T265_09755) (S1 and S2 Tables). These findings underscore the critical role of diverse signaling pathways in early developmental processes and successful host adaptation of juvenile *O. viverrini*, likely facilitating coordinated regulation of growth, differentiation, and environmental sensing during establishment in the host.

Our results in D14 worms further revealed up-regulated genes involved in energy metabolism including *Pyruvate dehydrogenase E1 component subunit alpha* (T265_07717), *Pyruvate dehydrogenase E1 component subunit beta* (T265_11829), *Dihydrolipoamide acetyltransferase component of pyruvate dehydrogenase complex* (T265_00275), *Succinate-CoA ligase [ADP/GDP-forming] subunit alpha*, *mitochondrial* (T265_00432), *Cytochrome* (T265_09703), *Cytochrome c domain-containing protein* (T265_09199), *Cytochrome c oxidase subunit 1* (T265_12110), and *ATP synthase subunit beta* (T265_01732) (S1 and S2 Tables). These expression patterns suggest an increased demand for pyruvate, likely coming from host environment, tricarboxylic acid (TCA) cycle activity, and oxidative phosphorylation in D14, consistent with

Table 2. Top up-regulated genes in D14 compared to D42 with log2FC > 3.

Gene ID	Log2FC	Adjusted p-value	Gene name
T265_11595	8.50	1.18E-10	Secreted protein
T265_11050	7.89	4.17E-33	Peptidase A1 domain-containing protein ^a
T265_11760	6.89	3.68E-05	Peptidase A1 domain-containing protein ^a
T265_10009	6.33	1.10E-04	C-type lectin domain-containing protein
T265_04509	6.13	7.19E-04	Homeobox domain-containing protein
T265_13674	6.13	7.53E-14	Peptidase A1 domain-containing protein ^a
T265_12117	5.88	2.28E-03	—
T265_05132	5.54	2.74E-03	BLOC-1-related complex subunit 5
T265_14809	5.44	7.17E-03	PI3K/PI4K domain-containing protein
T265_15271	4.88	3.54E-04	Tetraspanin
T265_07894	4.58	1.96E-04	Iron ABC transporter permease
T265_15680	4.46	4.90E-04	SMB domain-containing protein
T265_12094	4.34	1.04E-04	Legumain ^a
T265_10755	4.25	2.53E-05	Legumain ^a
T265_05905	4.23	4.46E-13	SERPIN domain-containing protein
T265_01174	4.15	7.69E-05	Usp domain-containing protein
T265_02179	4.06	3.16E-09	Periplasmic binding protein
T265_05858	3.98	1.39E-03	Cadherin domain protein
T265_11933	3.81	4.43E-05	Peptidase C13 family protein ^a
T265_03732	3.64	3.83E-03	Zinc finger, C2H2 type
T265_15287	3.59	9.90E-03	Ig-like domain-containing protein
T265_02178	3.56	1.27E-05	PLCXc domain-containing protein
T265_08985	3.56	1.38E-06	EF hand
T265_02180	3.49	6.21E-03	Usp domain-containing protein
T265_05750	3.48	1.27E-05	TGF_BETA_2 domain-containing protein
T265_09482	3.46	2.27E-36	Peptidase C13 family protein ^a
T265_03231	3.42	2.16E-06	Lipoyl-binding domain-containing protein
T265_03601	3.39	7.45E-03	G_PROTEIN_RECEP_F1_2 domain-containing protein
T265_12627	3.24	8.82E-04	PBPe domain-containing protein
T265_10342	3.17	5.91E-08	PDZ domain-containing protein
T265_10111	3.12	3.63E-12	SCP domain-containing protein
T265_10691	3.11	6.37E-05	G_PROTEIN_RECEP_F1_2 domain-containing protein
T265_15375	3.10	1.56E-52	Legumain ^a
T265_15407	3.08	5.38E-09	Legumain ^a
T265_12947	3.04	2.34E-06	guanylate cyclase
T265_15658	3.02	6.16E-06	PID domain-containing protein

^aGenes involved in the proteolysis of the *O. viverrini* in the developing juvenile stage (D14).

<https://doi.org/10.1371/journal.pntd.0013714.t002>

several enriched GO terms among the top 10, such as acetyl-CoA metabolic process, TCA cycle, electron transport chain, and proton motive force-driven ATP synthesis (Fig 4 and S4 Table). This highlights the energy-intensive nature of the early juvenile stage, reflecting a reliance on protein and carbohydrate metabolism for survival and maintenance.

The pairwise comparison between D42 and D180 adult worms showed only slight differences. Only five genes were considered significantly up-regulated in D42, and another five were up-regulated in D180 (S3 Table). The up-regulated genes at D42 included *H/ACA ribonucleoprotein complex subunit* (T265_11159), *Legumain* (T265_11946, T265_15375),

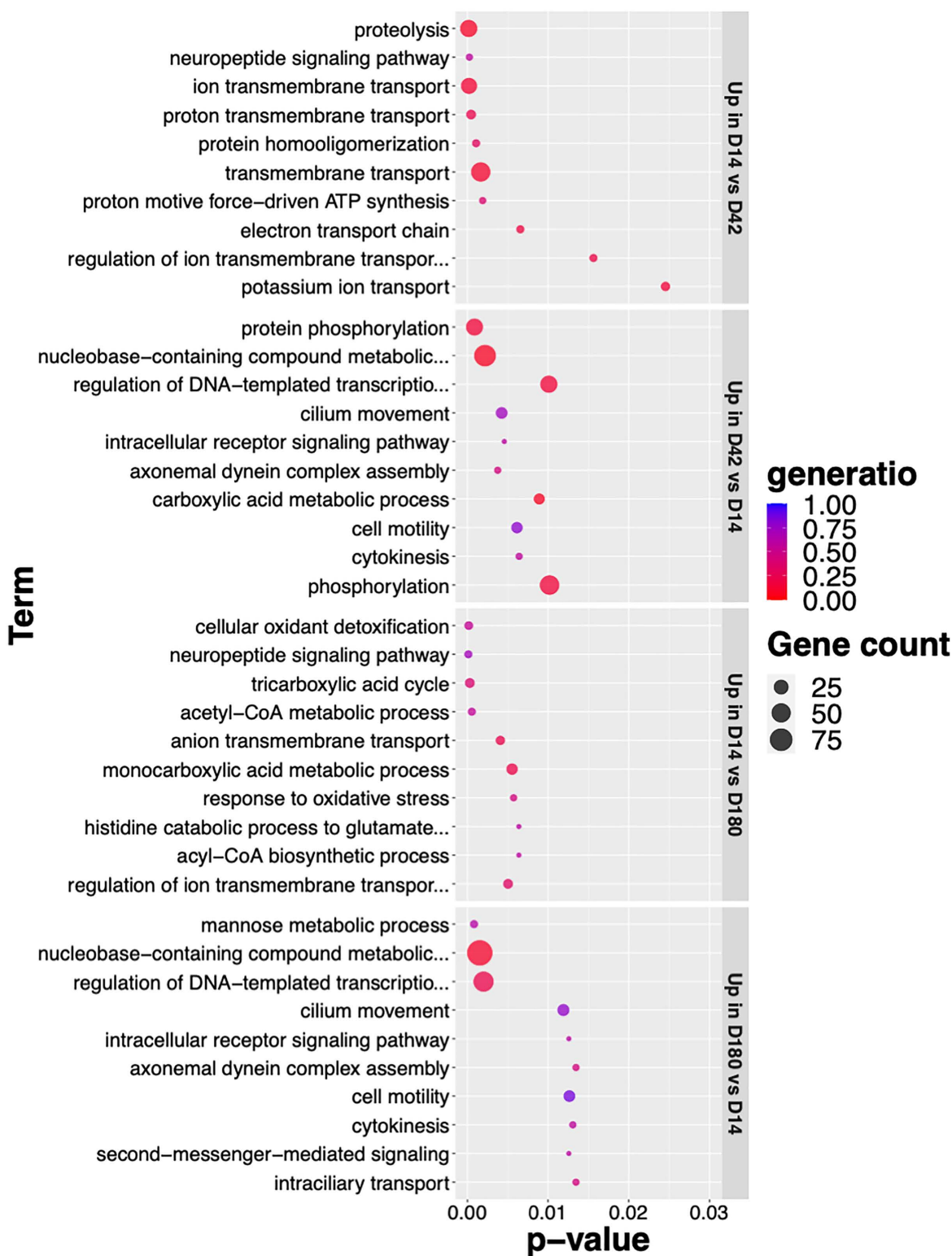


Fig 4. Top 10 enriched GO terms of up-regulated genes in the juvenile and adult stages. Only the biological process (BP) GO terms with p-value < 0.05 are shown, ranked by p-value. Dot size represents the number of genes associated with each BP term. Color represent gene ratio, i.e., the number of DEGs divided by the total number of genes annotated with the GO terms. The plot shows enriched biological processes of genes that

were up-regulated from four pairwise comparisons: D14 vs D42, D42 vs D14, D14 vs D180, and D180 vs D14. Detailed results of all enriched terms and associated up-regulated genes are available in [S4 Table](#).

<https://doi.org/10.1371/journal.pntd.0013714.g004>

TGF_BETA_2 domain-containing protein (T265_13153), and *Immunoglobulin domain protein* (T265_14313) ([S3 Table](#)). Four of these genes, excluding T265_11159, exhibited a declining expression pattern, with the highest expression observed at D14, followed by an approximately 2.5-fold decrease at each subsequent timepoint.

In contrast, the up-regulated genes at D180 in *O. viverrini*, associated with long-term infection included *L-ornithine N(5)-monooxygenase (NAD(P)H)* (T265_05877), *FHA domain-containing protein* (T265_06167), *Integrase catalytic domain-containing protein* (T265_10528), *Rho-GAP domain-containing protein* (T265_15550), and *Transcription elongation regulator 1* (T265_15863) ([S3 Table](#)). Again, all these genes demonstrated a steady increase in expression from D14 through D42 to D180, suggesting significant changes occurring in the parasites during chronic infection.

Mating system and host immune evasion at advanced life stages

Compared to the D14 juvenile worms, up-regulated genes in two adult stages (D42 and D180) showed, as expected, multiple genes potentially related to the parasite reproductive system. Given that this dataset came from pools of worms and their hermaphroditic nature, it is limited in describing the reproductive biology of the worms. However, their expression levels indicated that the gene expression patterns were consistently up-regulated in similar manners at both D42 and D180 compared to lower expression in D14 ([Fig 5](#)), emphasizing their likely roles in the reproductive stage of the parasite. These genes comprised of *Testis expressed 36* (T265_13259, T265_15840, T265_11057, T265_13259), *Meiosis-specific nuclear structural protein 1* (T265_12750), *Spermatogenesis associated 6 like* (T265_14145), *Sperm-associated antigen 6* (T265_01224), *Sperm-associated antigen 17* (T265_13031), *Ovule protein* (T265_13954, T265_03571, T265_10863), *Trematode Eggshell Synthesis* (T265_06163, T265_14710, T265_01554, T265_06806), *Tyrosinase* (T265_07190), *Tyrosinase_Cu-bd domain-containing protein* (T265_08937, T265_07191), and *M96 mating-specific protein* (T265_00841).

At D42 and D180, genes potentially related to host immune evasion were strongly up-regulated. In particular, a gene encoding *plasminogen* (T265_09328) showed a high expression level with log2FC greater than 12 (more than 4,000-fold increase) in both D42 and D180 conditions compared to the D14 group as clearly depicted in [Fig 6A](#), light blue line. Plasminogen is a zymogen (proenzyme) of plasmin, which contributes to the mechanism of fibrin destruction. By the work of plasmin and its interacting proteins, blood clotting and extracellular matrix (ECM) can be destroyed, and this process has been related to the escape from the host immune system [\[45\]](#).

Moreover, genes with potential binding interactions to plasminogen [\[45–47\]](#) were up-regulated in both adult stages in our transcriptomic data compared to the D14 group. These genes include *Actin* (T265_09603), *Adenylate kinase 8* (T265_11321), *Adenylate kinase isoenzyme 5* (T265_10351), *Adenylate kinase domain-containing protein* (T265_03321), and *Adenylate kinase 9* (T265_01856) – all of which were up-regulated by 2–5-fold ([Fig 6A](#) and [S5 Table](#)). One of the *Triosephosphate isomerase* (T265_10014) also narrowly passed the cut-off for the pairwise comparison between D14 and D180 worms with log2FC close to 1-fold ([S5 Table](#)). Although the expression of other genes encoding plasminogen-binding proteins was not significantly different between juveniles and adults in our study, many of these genes only narrowly missed the cut-off for either log2FC or adjusted p-value. These genes include *Glyceraldehyde-3-phosphate dehydrogenase* (GAPDH; T265_07589, T265_05806), *Glycerol-3-phosphate dehydrogenase* (T265_13416), *Phosphoglycerate mutase* (T265_13130, T265_03307), *Phosphoglycerate mutase family protein* (T265_02505), and one of the *Triosephosphate isomerase* (T265_10015) ([Fig 6B](#) and [S5 Table](#)). Some of these enzymes are multifunction proteins. For example, GAPDH is an important enzyme in glycolysis, but it has been shown to be a key player in host-parasite interactions from bacteria, fungi, to parasitic worm [\[48,49\]](#) specifically by binding to host plasminogen and disrupt immune

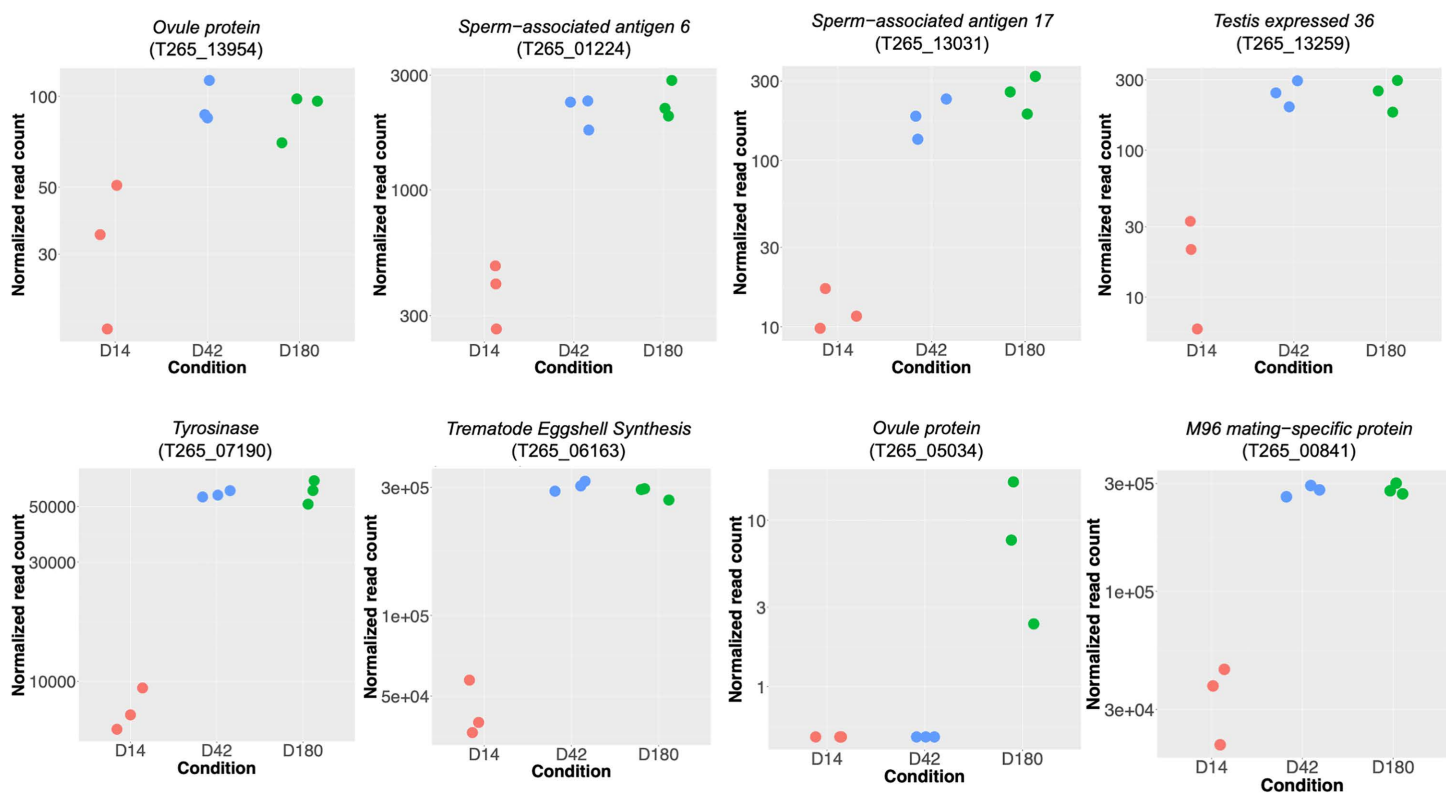


Fig 5. Gene expression of reproduction-related genes highly expressed in adult stages. Gene count plots show normalized read counts (DESeq2) of selected genes potentially involved in the reproductive system. Each dot represents a biological replicate.

<https://doi.org/10.1371/journal.pntd.0013714.g005>

invasion and blood-clot lysis. This important multifunction nature may explain the non-concordance level with plasminogen, and spectacularly high expression level.

Among the up-regulated genes with dramatic differential regulation revealed a group of *SCP-like protein* (T265_14885) and *SCP domain-containing proteins* (T265_02482, T265_15023, T265_04266, and T265_12675), with $\log_{2}FC > 10$ or greater than 1,024-fold in adult stages compared to juvenile (S6 Table). The SCP-domain containing protein, also known as cysteine-rich secretory protein/antigen 5/pathogenesis related-1 (CAP) or Sperm-coating protein/Tpx-1/Ag5/PR-1/Sc7 (SCP/TAPS) domains has been recognized as a key virulence factor in parasitic infection [50]. The exceptionally high expression of these genes in adult stages from our study in both acute and chronic infection suggested that the *SCP-like protein* and *SCP domain-containing proteins* might be playing critical biological roles in the *O. viverrini* biology and survival.

We further investigated the genes encoding SCP domain-containing proteins in *O. viverrini* by pulling expression profile of other genes in this family based on annotated protein domain (Pfam ID PF00188 and InterPro ID IPR014044) [50]. A total of 25 SCP/TAPS genes were found from reference genome of *O. viverrini* (Fig 7 and S6 Table). Note that there are other genes annotated as SCP domain containing protein or SCP-like protein; however, some of these genes were not assigned with the established protein domain ID associated with SCP/TAPS and therefore not included in our investigation. Of the 25 SCP/TAPS genes investigated, ten were express at very low level during the intra-mammalian stages in this study, rendering noisy data and insignificant adjusted p-value (Fig 7, uppermost cluster). Three of these showing no detectable reads at all. The rest seem to be expressed throughout the whole timecourse, but the level was shifting

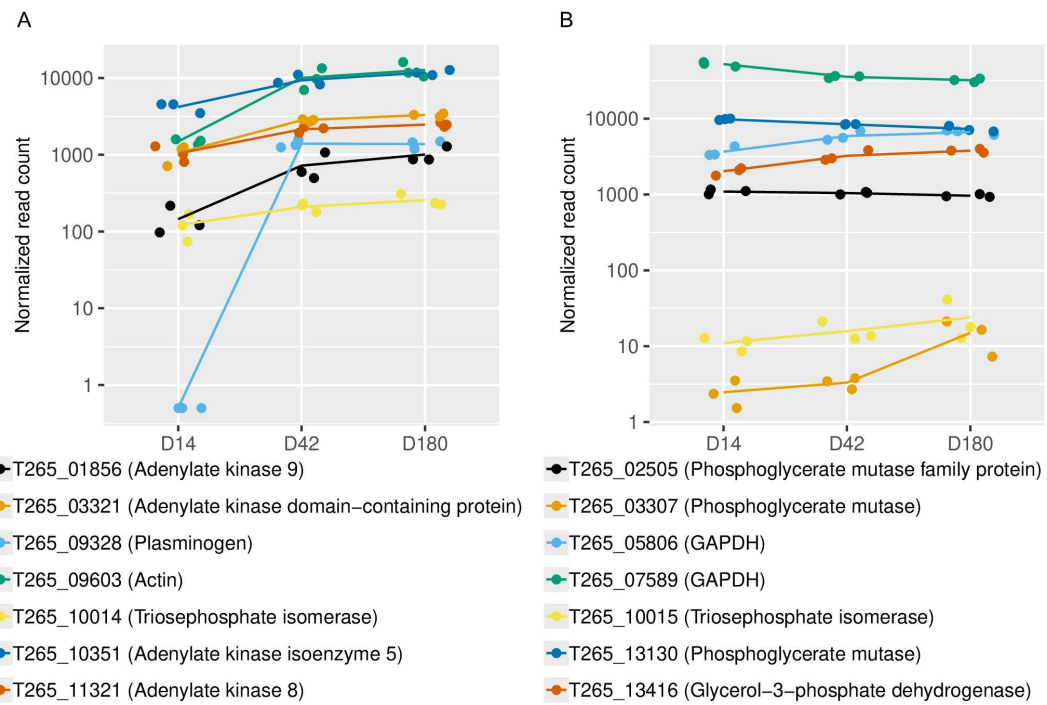


Fig 6. Expression of plasminogen and plasminogen-binding protein. Normalised counts of genes encoding plasminogen and plasminogen-binding proteins over the timecourse. Color represents different gene ID as shown under each panel. Gene descriptions are based on annotation from *O. viverrini* reference genome [17] on WBPS19. **A)** Genes that were up-regulated in at least one adult stage compared to D14 juvenile. **B)** Genes that were not considered up-regulated in adult stages compared to D14 juvenile. Details of log2FC and adjusted p-value for each pairwise comparison are available in [S5 Table](#).

<https://doi.org/10.1371/journal.pntd.0013714.g006>

between timepoints. In particular T265_15685, show the highest expression throughout all three timepoints with the level dropped slightly at D180 (~ 3-fold compared with D14 and ~2 fold compared with D42). Most differentially expressed SCP/TAPS were up-regulated in the adult stages (both D42 and D180) (Fig 7, turquoise annotation), while some were highly expressed in D14 and reduced in expression down in adult worms (Fig 7, yellow annotation). This data emphasized SCP/TAPS genes that may be important for intramammalian infection, with some specific to juvenile or adults, and provide novel revenue for future investigation.

In advanced developmental stages (D42 and D180 compared to D14), up-regulation of other genes encoding products potentially related to immune interactions were observed. These include *Ig-like domain-containing protein* (T265_01038, T265_10657), *IL4_i_Ig domain-containing protein* (T265_01060), *Peptidase_M24 domain-containing protein* (T265_12477), and *Peptidase_M13_N domain-containing protein* (T265_12599, T265_15775) (S1 and S2 Tables). Some of these genes have orthologs in other parasitic fluke species, including *Opisthorchis felineus*, *Clonorchis sinensis*, and *Fasciola hepatica* (S7 Table), suggesting their potential roles in host-parasite interactions.

Potential drug targets among cell surface receptors in juvenile and adult *O. viverrini*

At D14, almost 20 up-regulated genes were annotated as cell surface receptor annotated as *G_PROTEIN_RECEP_F1_2 domain-containing protein* (T265_03601, T265_10691, T265_02329, T265_01275, T265_03494, T265_02724, T265_00716, T265_00683, T265_09662, T265_14292, T265_08353, T265_11536, T265_01578, T265_06423, T265_01985, T265_00777, T265_02701) (S1 and S2 Tables). GO enrichment results support the inference that the majority of these GPCRs were involved in neuropeptide signaling pathway, and G protein-coupled peptide receptor

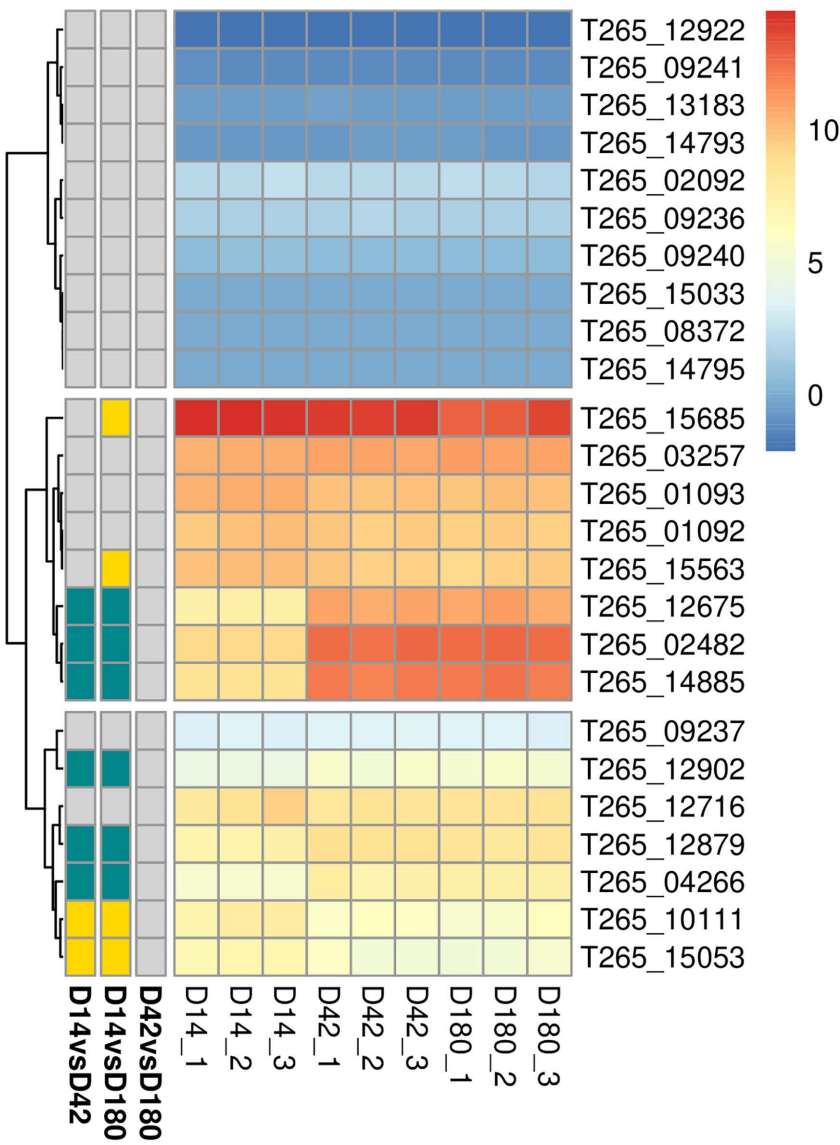


Fig 7. Hierarchical clustering of SCP/TAPS genes based on expression level over the timecourse. Heatmap color represent rlog-transformed values of SCP/TAPS genes that were assigned with protein family ID PF00188 (Pfam) and IPR014044 (InterPro). Annotation on the left indicated results of pairwise comparison ($\log_{2}\text{FC} > 1$ or < -1 , and adjusted p -value < 0.01). Yellow indicates up-regulation in earlier timepoint (e.g., up-regulated in D14 compared to D42); turquoise indicates up-regulation in later timepoint; grey indicates not passing the cut-offs for differential expression. Details of $\log_{2}\text{FC}$ and adjusted p -value for each pairwise comparison and based mean expression level are provided in [S6 Table](#).

<https://doi.org/10.1371/journal.pntd.0013714.g007>

activity ([Fig 4](#) and [S4 Table](#)). In addition, the enriched GO term ion transmembrane transport contained 31 up-regulated genes in D14 worms, such as *ATPase protein 9*, *ATP synthase subunit beta*, *BTB domain-containing protein, Amiloride-sensitive sodium channel*, *Glycine receptor subunit beta-type 4*, *Calcium-transporting ATPase*, *Amino acid transporter*, *Neurotransmitter-gated ion-channel*, *Otopetrin*, and *Cytochrome c oxidase subunit 1* ([S4 Table](#)). GPCRs are known to be effective pharmacological targets in a various biological system. These upregulated GPCRs and ion channels may affect the parasite's neuromuscular functions, sensory perceptions, or ability to absorb molecules from host, providing a rational basis for the development of antiparasitic medications.

In D42 and D180 worms, some *nuclear receptor domain-containing protein* (T265_09674, T265_15765) were revealed in enriched GO term related to transcriptional regulation and DNA-binding and nucleobase-containing compound metabolism (Fig 4 and S4 Table), suggesting roles in stage-specific gene expression regulation. In parallel, multiple genes related to protein phosphorylation and signaling pathway regulation were also up-regulated in D42 and D180, including *receptor protein-tyrosine kinases* (T265_03081 and T265_02140) in D14, and *protein-tyrosine phosphatases* (T265_10810, T265_10484, T265_01620, T265_13563, T265_13236) (S1 and S2 Tables). Consistently, the top enriched GO terms at D42 and D180 included protein phosphorylation, representing many members of *protein kinase domain-containing proteins* (Fig 4 and S4 Table). These findings point to dynamic regulatory processes during parasite maturation and chronic infection, and further highlight candidate genes, particularly kinases, phosphatases, and nuclear receptors, which have been established as drug targets in oncology and immunomodulation, where a range of small-molecule inhibitors is already available.

GSEs across the life stages of *O. viverrini* in the hamster model

While differentially expressed genes highlight stage-specific changes and putative virulence factors in *O. viverrini*, identifying genes consistently expressed across intramammalian stages may reveal novel diagnostic biomarkers and further identify drug targets. To investigate GSEs, raw gene count values were converted to TPM, and CV were calculated for each gene across all replicates of all timepoints. As a result, a total of 2,011 *O. viverrini* genes passed the criteria for GSEs ($CV \leq 0.15$), indicating that these GSEs were constitutively expressed across all nine samples. However, as demonstrated on the heatmap, the level of expression varied with a few genes expressed at exceptionally high levels and the majority showing relatively low expression (Fig 8).

Notably, we conducted the GO enrichment analysis to comprehend all fundamental cellular processes derived by GSEs that impact to the parasite biology. The GO enrichment analysis of GSEs revealed around total hundred terms related to biological processes (BP), molecular functions (MF), and cellular component (CC) (S9 Table). In terms of BP, the GSEs were associated with the fundamental flow of genetic information from DNA to RNA to protein such as DNA replication and mRNA processing. Some of the top-scoring enriched BP were related to RNA metabolisms and modification. In addition, the transport of cellular materials and biological molecules was evidently noted in BP, such as protein transport, Golgi vesicle transport, exocytosis. Additionally, the regulation of cell cycle and cellular response were also observed (Fig 9 and S9 Table). Our data suggest that all these biological processes are crucial for *O. viverrini* during their intra-mammalian development.

Of a total 2011 GSE, those with potential value as biomarkers for diagnosis or novel candidate for drug targets were identified based on existence of gene orthologs in other relevant species including human host, and closely related trematode *O. felineus*, *C. sinensis*, *F. hepatica*, and common co-infection agent *Strongyloides stercoralis* (Fig 10 and S8 Table). The highest number of GSE orthologs were found from *O. felineus*, followed by *C. sinensis*, both of which are closely related trematodes, and followed by *F. hepatica*, another liver fluke. This pattern is consistent with phylogenetic relationships. Interestingly, more GSE orthologs were shared with humans than with *S. stercoralis*, a parasitic nematode. A likely explanation is that *S. stercoralis* has a small genome (~43 Mb), compared to trematode such as *O. viverrini*, *O. felineus*, *C. sinensis*, and *F. hepatica* (~500–2000 Mb) and has undergone substantial gene loss and divergence, especially in conserved pathways, as part of its specialized parasitic lifestyle. As a result, its compact genome and annotation limitations may reduce detectable orthologs. Comparative genomics of major parasitic worms have demonstrated that variations in genome size influence gene contents, resulting in many gene families being highly diverged where ancestry is difficult to traced [51]. Furthermore, evolutionary analysis demonstrated that gene loss is less captured in *Lochotrophozoa* (which includes platyhelminthes) than *Ecdysozoa* (which includes nematodes) [52]. This low GSE conservation is also reflected by the evolutionary distance separating *Lophotrochozoa* and *Ecdysozoa*.

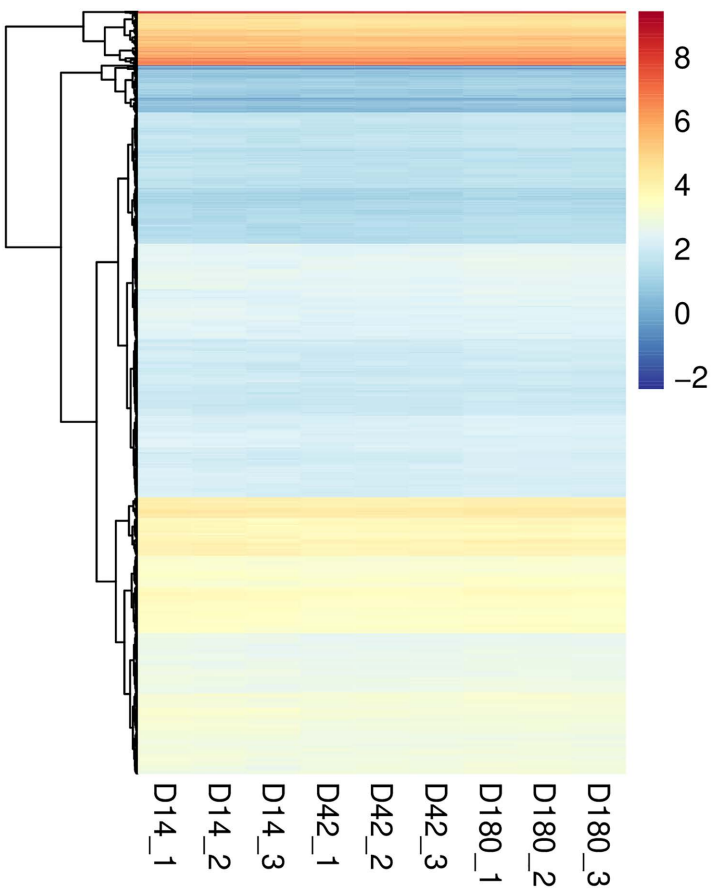


Fig 8. Novel 2,011 GSEs in *O. viverrini* during intramammalian infection. GSEs are those with $CV \leq 0.15$ across all nine samples (three timepoints, three replicate each). Color of the heatmap represent log TPM. The X-axis showed different sample groups, the Y-axis represent the identified GSEs. Full details with gene IDs, gene description, TPM, and CV values are provided in [S8 Table](#).

<https://doi.org/10.1371/journal.pntd.0013714.g008>

We identified 137 GSEs with no detectable orthologs in any of the species examined (Fig 10 and S8 and S10 Tables). *S. stercoralis* was included due to its common co-endemicity with *O. viverrini* in rural areas, where populations are frequently exposed to soil and natural water sources. These 137 uniquely expressed genes could serve as specific targets for *O. viverrini* detection by protein antigen-based diagnostics – an approach already validated and approved by the Thai FDA and used in field settings [11]. These genes warrant further investigation, including proteomic profiling or validation using archived or prospective samples from infected individuals. On the other hand, for drug target development, GSEs conserved across multiple fluke species may be more valuable, as three trematodes (*O. viverrini*, *O. felineus*, and *C. sinensis*) are currently treated with praziquantel, with risk of reduced efficacy in regions with heavy use. To this end, we highlighted 267 constitutively expressed GSEs that are conserved in other liver fluke species as potential multi-species drug targets (Fig 10 and S8 and S11 Tables).

Expression of these genes could be useful information inferring the suitability as a diagnostic biomarker. We, therefore, clustered the genes found in the *O. viverrini*-only group (137 genes) and identified some groups of highly expressed genes (Fig 11A and S10 Table); for example, *RRM domain-containing protein* (T265_16372 (645.87 TPM)), *eIF3g domain-containing protein* (T265_16333 (723.07 TPM)), *LIM domain protein* (T265_14316 (384.14 TPM)), and *Fibronectin type-III domain-containing protein* (T265_00431 (22.01 TPM)). There were, however, genes with apparently high TPM but

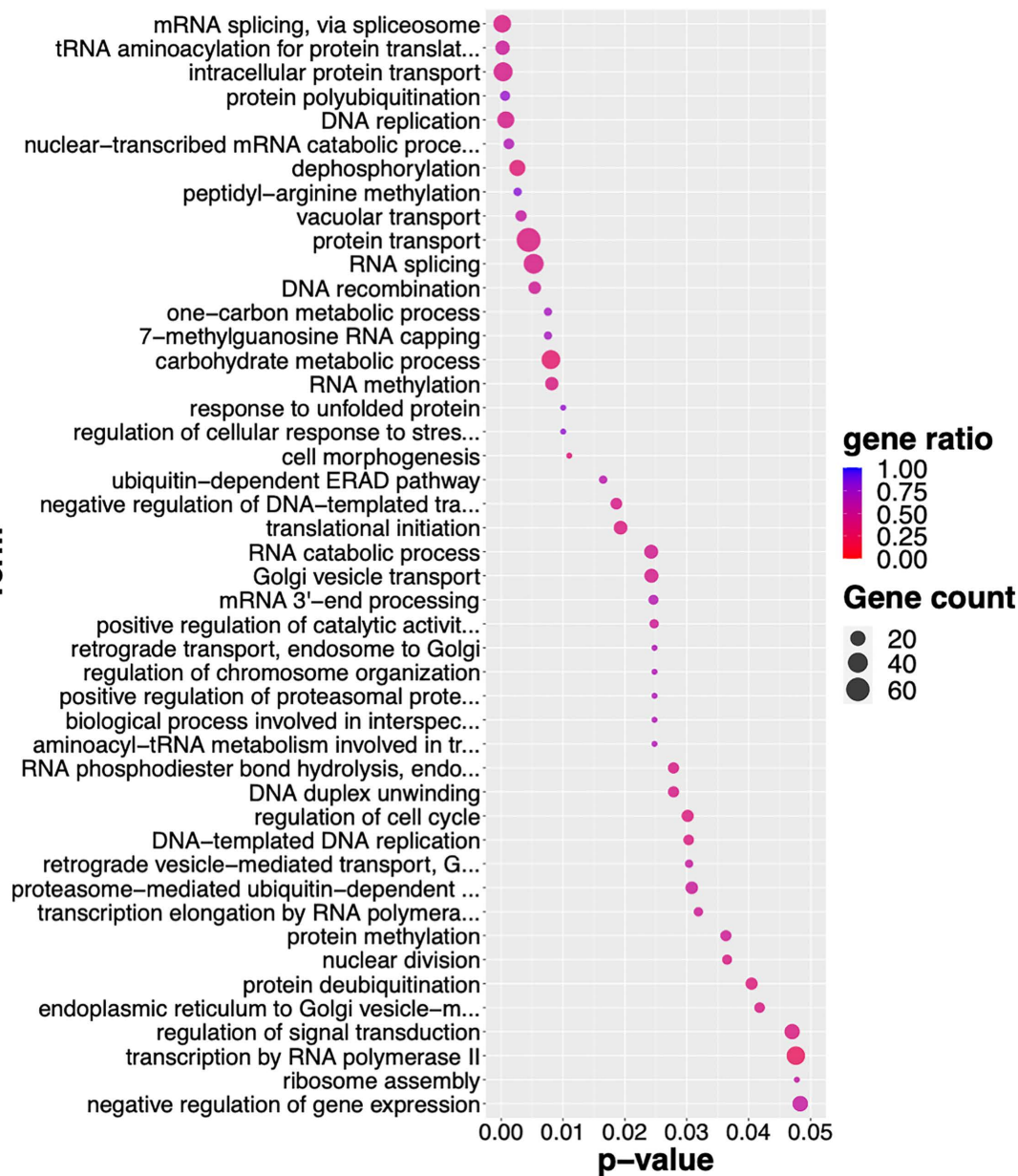


Fig 9. Enriched GO terms of GSEs. Only biological process terms with $p\text{-value} < 0.05$ are shown, ranked by $p\text{-value}$. Dot size indicates the number of genes associated with each GO term. Color represents gene ratio which is the number of GSEs divided by the total number of genes annotated with each GO term. Detailed results of all enriched terms and associated GSEs are available in [S9 Table](#).

<https://doi.org/10.1371/journal.pntd.0013714.g009>

without annotated description. Some of these genes, T265_13159 (3528.37 TPM) and T265_15973 (3695.81 TPM) for examples, are relatively short and maybe misannotated. Others without annotated description, however, could be of interest; for example, T265_12203 (229.47 TPM) and T265_04304 (457.56 TPM) consist of transmembrane domain and may be exposed to host environment and thus could serve as good candidates for diagnostic biomarkers. Genes with signal peptide suggested that they may be released into host environment, such as T265_10887 (19.21 TPM) and T265_11396 (annotated as *lysosome-associated membrane glycoprotein 2*, 7.04 TPM) and may serve as diagnostic biomarkers.

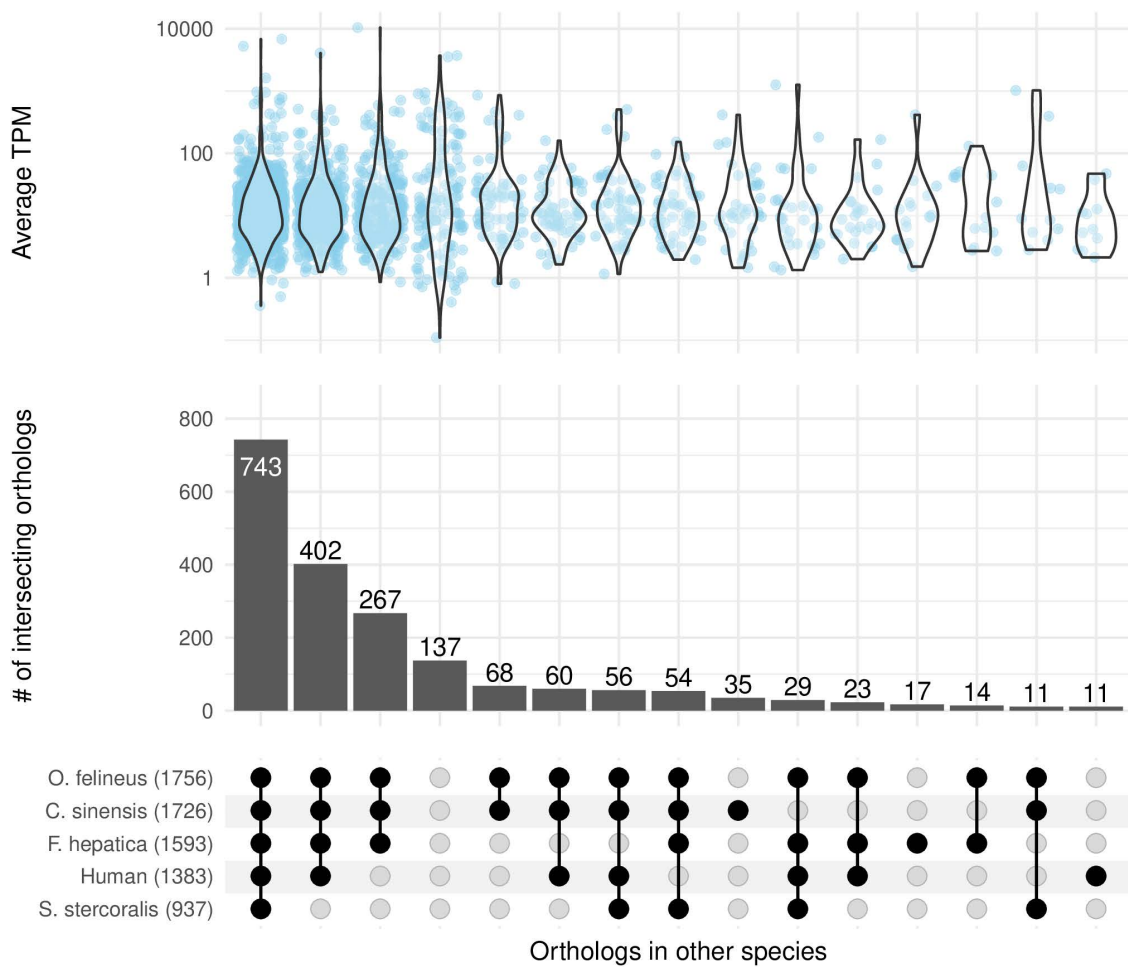


Fig 10. Shared orthology in GSEs. The bottom upset plot shows presence of GSEs in *O. viverrini* in other relevant species – human, *O. felineus*, *C. sinensis*, *F. hepatica*, and *S. stercoralis* – as indicated by black dots. The number after each species names indicates the total number of orthologs found among the 2,011 GSEs in *O. viverrini*. The correspondent bar chart indicates the number of intersecting orthologs across species. The upper violin plot represents distribution of GSE expression level in our *O. viverrini* data shown as average TPM from all replicates of all timepoints. The identification of inter-species orthology was based on available public data provided by WBPS19 [33]. Details of gene IDs and gene descriptions in *O. viverrini* and correspondent orthologs are available in [S8 Table](#).

<https://doi.org/10.1371/journal.pntd.0013714.g010>

Likewise, genes with potential value as novel drug targets – shared among related liver flukes – also show varying expression level (Fig 11B and S11 Table). Of the 267 genes, identified as having shared orthologs with other liver fluke species but not with humans, several of these genes are involved in critical cellular processes such as RNA transcription, protein stability, and enzymatic activity, which are crucial for the survival and pathogenicity of parasitic flukes. Notably, some of these genes encode enzymes that have known repurposable drugs, suggesting their relevance for therapeutic targeting; for instance, *cytochrome P450* (T265_00657) and *fatty acid synthase* (T265_01246) [53]. Additionally, the clusters of expression level of these genes (S11 Table) offer insights into their functional roles and relevance for drug development. Targeting these conserved genes could pave the way for broad-spectrum treatments against parasitic flukes, improving therapeutic options across multiple species.

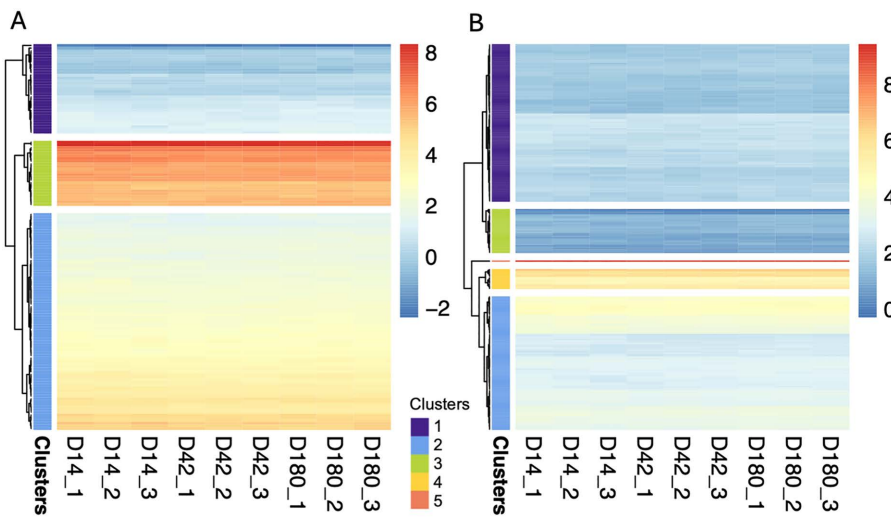


Fig 11. Clusters by expression level of GSEs. Color of the heatmaps represents log-transformed TPM. Cluster numbers were assigned internally during hierarchical clustering. **A)** Expression level of GSEs with no detectable orthologs in any of the species examined. **B)** Expression level of GSEs conserved in other liver fluke species. Details on the expression levels of each GSE (average TPM) and the grouping cluster they belong to are provided in [S10](#) and [S11 Tables](#).

<https://doi.org/10.1371/journal.pntd.0013714.g011>

Discussion

In this study, we presented a comprehensive transcriptome analysis of *O. viverrini* to identify differentially expressed genes associated with the parasite developmental milestones within mammalian host. Notably, the up-regulation of genes involved in energy metabolism, and signaling pathways inferred mechanisms supporting the parasite's survival and growth within the liver of hamsters. In adult stage, we revealed key up-regulated genes that might be influenced the mating and reproduction, suggesting the molecular basis for the parasite's reproductive success in a monoecious organism. Additionally, our analyses revealed the expression of genes involved in host defense mechanisms, providing insights into the parasite's strategies for evading the host immune response. For the first time, the GSEs of Asian liver fluke were explored in our study using RNA-seq analysis that include parasites from a chronic infection. These GSEs represented potential candidate genes for diagnostic applications and development of novel intervention against *O. viverrini* and related liver fluke infection. The challenge of our transcriptomic profiling was that some intermediate mRNAs might not be produced as functional proteins depending on many factors, such as mRNA isoforms, alternative splicing, post-translation modification. As a result, the technologies of protein-based identification could be further implemented using additional *in vivo* specimen.

During the development of juvenile (D14), diverse peptidase genes related to proteolysis were considered to promote the evasion of host immune system and parasite feeding [54]. However, it could also be related to developmental period of the parasites as multiple genes related to signalling and differentiation were also up-regulated. *Homeobox* genes, or well-known as *Hox*, are associated with growth and development by acting as transcription factors [55] in model organism as well as in parasitic worm, such as *Drosophila melanogaster* (fruit fly) and *Schistosoma mansoni* (human blood fluke) [56]. High expression of *PI3K domain-containing protein* has been described previously in *F. hepatica* at immature liver stage, responding for rapid differentiation and proliferation of stem cells [57]. Up-regulated *guanylate cyclase*, *cAMP-dependent protein kinase*, and *TGF-β domain-containing protein* in juvenile worms from our dataset infer a wide range of cellular functions, including signal transduction in cell growth and development via second messenger molecules, cAMP and cGMP [58]. For instance, in *C. elegans*, cGMP and TGF-β signaling play roles in regulation of behavior of food intake [59].

Multiple signaling-related genes were up-regulated in juvenile *O. viverrini*, and these have been proposed as drug targets as listed in the study of *S. mansoni* genome and *Taenia pisiformis* transcriptome, such as GPCRs, voltage-gated ion channels, kinases, and neuropeptides [38,60]. Specifically, inhibitory small molecules against certain proteases tends to be developed as potential vaccine targets for the prevention of helminth infection [61]. Our RNA-seq data revealed many up-regulated genes in each developmental stages with roles in cell signaling. These candidate genes could contribute as drug or vaccine targets, resulting in the interruption of many internal signal transduction pathways as well as terminating the important biological functions in *O. viverrini*.

At more advanced life stage (D42 and D180), up-regulation of multiple reproductive genes is consistent with the mature stage of the parasite. Transcriptomic profiling of the *S. mansoni* found the eggshell production-related genes which were *tyrosinase* and *egg shell protein* being up-regulated in adult human blood fluke [39]. Another work using the RNA-seq data of *S. mansoni*, revealed that *tyrosinase* was proposed as a component of eggshell synthesis [62]. Surprisingly, a gene encoding *ovule protein* showed low expression level in the juvenile stage despite the worms supposedly being reproductively inactive. This might be a novel information of *O. viverrini* relating to its egg production prior to fully mature adult stage, or the gene may have multiple functions. Moreover, this information may offer an alternative strategy for intervention aimed at parasite burden control by focusing on reproductive biology as demonstrated in species like *S. mansoni* [63].

Multiple genes encoding SCP domain-containing proteins showed extremely high expression levels at D42 and D180 compared to the juveniles, and suggested candidate SCP/TAPS proteins that maybe important for chronic infection of *O. viverrini*. According to related studies, diverse SCP/TAPS proteins in parasitic helminth species were identified. For example, *venom allergen homologue asp-like 1* (GenBank accession number: AF334661) in *Brugia malayi* contains a single SCP-domain and is involved in mammalian host invasion process [50,64]. Additionally, in *Ancylostoma caninum*, two secreted proteins with SCP/TAPS domain (secreted protein-2 (GenBank accession number: Q16937) and secreted protein-3 (GenBank accession number: AY217004) are involved in pathogen recognition during infection process and maintenance of host-parasite interaction [64]. Notably, the proteomic analysis in hookworm, *Necator americanus* revealed proteins sharing SCP domain-containing proteins, such as NAME_01772 (asp1 (SCP-like protein)), NAME_01050 (SCP domain-containing protein), and NAME_06207 (CAP superfamily) that might be associated with functional roles of SCP/TAPS family [65].

Significantly and strongly up-regulated in both adult stages compared to the juvenile stage included a gene encoding *plasminogen* (T265_09328) and some putatively plasminogen-binding proteins. Plasminogen has been studied for their crucial roles in host immune response in other species of trematode, particularly for its fibrinolytic and host immune evasion activity. In *Schistosoma bovis*, tegument extracts of mature male worm were able to increase plasmin production similar to tissue-type plasminogen activator. Their proteomic results revealed ten plasminogen-binding proteins [47]. During the adult stage of sheep liver fluke (*F. hepatica*), the expression of *plasminogen-binding protein* degraded blood clotting via action of bradykinin, resulting in host inflammation and chronic fascioliasis [46]. What is more, the investigation of *serine protease 2* in *S. mansoni* secretome suggest the tendency of converting plasminogen to plasmin by the parasite, which in turn affect thrombolysis, and modulate host immune defense via anti-hemostatic properties [66].

Principle component analysis revealed that the two adult stages (D42 vs D180) differ by only 2% of the variance, indicating minimal transcriptomic changes during chronic infection. Consistent with this, only 10 genes were differentially expressed between the two stages, suggesting that adult *O. viverrini* maintain largely stable gene expression profiles once maturity is reached. Minor expression changes, such as up-regulation genes related to RNA processing (*H/ACA ribonucleaseprotein complex subunit*) and immunomodulation (*legumain*, *TGF- β 2-domain containing protein*, and *immunoglobulin domain protein*) may reflect subtle host-parasite interactions rather than major developmental transitions. These findings support the notion that factors beyond the parasite's life cycle development, such as host immune state or tissue microenvironment, may contribute more substantially to chronic infection outcomes [67].

To identify candidate genes for liver fluke intervention, we identified over 2,000 GSEs that were constitutively expressed during mammalian infection. Of these, the most abundance proteins comprised genes encoding *tubulin*, *heat shock protein 90 (HSP90)*, and *fructose-bisphosphate aldolase*. These proteins was suggested as vaccine targets with high antigenic activity in fish ectoparasitic flatworm (monogeneans) [68]. *Tubulin-specific chaperone D* in *O. viverrini* is highly similar to that of *F. hepatica*, *C. sinensis*, and *O. felineus*, but with low percent identity to human [33]. This gene also have the constant expression level in all developmental phases of *F. hepatica* [69], suggesting its value as potential new drug or diagnostic candidate against liver flukes. Moreover, our identified GSEs could be employed as reference gene in quantitative assays such as RT-qPCR. A gene *cAMP-dependent protein kinase* was suggested as reference gene of tapeworm, *Hymenolepis microstoma*, for the gene quantification by RT-PCR. It was found to be more suitable for comparison with low-expression genes, such as *Hox*, because its Ct values is relatively close to that of *Hox*, resulting in less potential confounding effect when using high-expression genes such as *18S rDNA* as a reference control [70]. It worth emphasizing that our list of GSEs provide genes covering a range of expression level, which can be utilized appropriately as a reference for genes of interest.

Our study provides novel insights into the biology of *O. viverrini*, spanning from the juvenile stage to the acute- and chronic-infected adult stages within mammalian hosts. Transcriptomic analysis revealed numerous stage-specific genes that are critical for the survival and development of *O. viverrini*, highlighting potential therapeutic targets for disrupting key biological processes and advancing diagnostic applications. Furthermore, the identification of genes with previously unknown functions underscores the informed opportunity for future investigations to explore their roles in parasite biology. Overall, this work enhances our understanding of the molecular landscape of *O. viverrini* and establishes a valuable foundation for the development of innovative diagnostic and preventative strategies against opisthorchiasis.

Conclusion

In conclusion, our RNA-seq analysis of intra-mammalian stages *O. viverrini* has significantly expanded our understanding of the parasite's biology across its developmental stages. By investigating the gene expression profile, we have identified key up-regulated genes in biological processes, including energy metabolism, proteolysis, signaling pathways, and growth and development. Furthermore, our findings have revealed numerous genes associated with the parasite's survival within the mammalian host, including those involved in evading and interacting with the host immune response. Notably, we identified 2,011 genes with stable expression, essential for maintaining cellular functions, some of which are uniquely present in non-human species. The transcriptomic data from this study not only provide a deeper understanding of *O. viverrini* infection, but also offer a valuable resource to support future research and development of anthelmintic targets and diagnostic markers for *O. viverrini* and other related parasitic worms.

Supporting information

S1 Table. Pairwise comparison of differentially expressed genes between D14 and D42.
(XLSX)

S2 Table. Pairwise comparison of differentially expressed genes between D14 and D180.
(XLSX)

S3 Table. Pairwise comparison of differentially expressed genes between D42 and D180.
(XLSX)

S4 Table. GO enrichment results of up-regulated genes in each condition.
(XLSX)

S5 Table. Log2FC and adjusted p-value of plasminogen and genes previously proposed or characterized as plasminogen-binding protein in *O. viverrini* or related species.

(XLSX)

S6 Table. Log2FC and adjusted p-value of SCP/TAPS genes (PF00188 (Pfam) and IPR014044 (InterPro)).

(XLSX)

S7 Table. Orthologues of *O. viverrini* immune-related genes in *O. felineus*, *C. sinensis*, and *F. hepatica*.

(XLSX)

S8 Table. TPM, CV, and orthology information of 2,011 GSEs in *O. viverrini* during infection in the mammalian host.

(XLSX)

S9 Table. GO enrichment results of GSEs.

(XLSX)

S10 Table. Expression level and cluster grouping of GSEs with no detectable ortholog in any of the species examined.

(XLSX)

S11 Table. Expression level and cluster grouping of GSEs conserved in other liver fluke species.

(XLSX)

S1 File. Coding sequence counts for DEG analysis. The HTSeq-count data in the zipped folder contains the following files: ov_reads_D14_1_cds.txt, ov_reads_D14_2_cds.txt, ov_reads_D14_3_cds.txt, ov_reads_D42_1_cds.txt, ov_reads_D42_2_cds.txt, ov_reads_D42_3_cds.txt, ov_reads_D180_1_cds.txt, ov_reads_D180_2_cds.txt, ov_reads_D180_3_cds.txt.

(ZIP)

Acknowledgments

We extend our gratitude to Mr. Taweesak Sarnboon for his assistance with parasite collection and host infection procedures, and to Associate Professor Nisarat Tungpairojwong for providing materials for RNA extraction optimization. We thank all members of the Systems Biosciences lab, the Department of Systems Biosciences and Computational Medicine, and the Department of Biochemistry, Faculty of Medicine, Khon Kaen University, and the Department of Biology, Faculty of Sciences, Khon Kaen University for their valuable support. The IT infrastructure for computationally intensive data analysis were supported by the Office of Digital Technology, Khon Kaen University. Appreciation is given to Wellcome Connecting Science for providing the Helminth Bioinformatics training course. Lastly, we thank all providers of databases and tools - WormBase Parasite, InterPro Scan, UniProt, NCBI, BLAST, and AlphaFold3 for open access to their data and tools.

Author contributions

Conceptualization: Arporn Wangwiwatsin.

Data curation: Waraporn Taweesin, Siriyakorn Kulwong.

Formal analysis: Waraporn Taweesin, Siriyakorn Kulwong.

Funding acquisition: Nisana Namwat, Watcharin Loilome, Arporn Wangwiwatsin.

Investigation: Waraporn Taweesin, Siriyakorn Kulwong, Wassana Jamnongkan, Wichit Taron, Autchasai Siriprayong, Sirinya Sitthirak, Anchalee Techasen, Nisana Namwat, Poramate Klanrit, Arporn Wangwiwatsin.

Methodology: Siriyakorn Kulwong, Wassana Jamnongkan, Wichit Taron, Autchasai Siriprayong, Sirinya Sitthirak, Anchalee Techasen, Opal Pitaksakulrat, Watcharin Loilome, Arporn Wangwiwatsin.

Project administration: Siriyakorn Kulwong, Watcharin Loilome, Arporn Wangwiwatsin.

Resources: Sirinya Sitthirak, Anchalee Techasen, Nisana Namwat, Poramate Klanrit, Watcharin Loilome, Arporn Wangwiwatsin.

Supervision: Anchalee Techasen, Nisana Namwat, Poramate Klanrit, Watcharin Loilome, Arporn Wangwiwatsin.

Validation: Waraporn Taweesin, Arporn Wangwiwatsin.

Visualization: Waraporn Taweesin.

Writing – original draft: Waraporn Taweesin.

Writing – review & editing: Nisana Namwat, Poramate Klanrit, Watcharin Loilome, Arporn Wangwiwatsin.

References

1. Khuntikeo N, Titapun A, Loilome W, Yongvanit P, Thinkhamrop B, Chamadol N, et al. Current perspectives on opisthorchiasis control and cholangiocarcinoma detection in Southeast Asia. *Front Med (Lausanne)*. 2018;5:117. <https://doi.org/10.3389/fmed.2018.00117> PMID: 29765958
2. Sithithaworn P, Yongvanit P, Duenngai K, Kiatsoptit N, Pairojkul C. Roles of liver fluke infection as risk factor for cholangiocarcinoma. *J Hepatobiliary Pancreat Sci*. 2014;21(5):301–8. <https://doi.org/10.1002/jhbp.62> PMID: 24408775
3. Sripa B, Kaewkes S, Sithithaworn P, Mairiang E, Laha T, Smout M, et al. Liver fluke induces cholangiocarcinoma. *PLoS Med*. 2007;4(7):e201. <https://doi.org/10.1371/journal.pmed.0040201> PMID: 17622191
4. Thinkhamrop K, Suwannatrat K, Kelly M, Suwannatrat AT. Spatial analysis of cholangiocarcinoma in relation to diabetes mellitus and *Opisthorchis viverrini* infection in Northeast Thailand. *Sci Rep*. 2024;14(1):10510. <https://doi.org/10.1038/s41598-024-61282-1> PMID: 38714779
5. Buathong S, Charoensuk L, Suwannahitatorn P. The past and present situation of *Opisthorchis viverrini* infection in Thailand. *Vajira Med J*. 2024:e267381. <https://doi.org/10.62691/vmj.2024.267381>
6. Zhao T-T, Feng Y-J, Doanh PN, Sayasone S, Khieu V, Nithikathkul C, et al. Model-based spatial-temporal mapping of opisthorchiasis in endemic countries of Southeast Asia. *Elife*. 2021;10:e59755. <https://doi.org/10.7554/elife.59755> PMID: 33432926
7. Pechdee P, Chaiyasaeng M, Sereewong C, Chaiyos J, Suwannatrat A, Wongmaneeprateep S, et al. Effects of albendazole, artesunate, praziquantel and miltefosine, on *Opisthorchis viverrini* cercariae and mature metacercariae. *Asian Pac J Trop Med*. 2017;10(2):126–33. <https://doi.org/10.1016/j.apjtm.2017.01.019> PMID: 28237476
8. Saengsawang P, Promthet S, Bradshaw P. Reinfection by *Opisthorchis Viverrini* after treatment with praziquantel. *Asian Pac J Cancer Prev*. 2016;17(2):857–62. <https://doi.org/10.7314/apjcp.2016.17.2.857> PMID: 26925692
9. Worasith C, Kamamia C, Yakovleva A, Duenngai K, Wangboon C, Sithithaworn J, et al. Advances in the diagnosis of human opisthorchiasis: development of *Opisthorchis viverrini* antigen detection in urine. *PLoS Negl Trop Dis*. 2015;9(10):e0004157. <https://doi.org/10.1371/journal.pntd.0004157> PMID: 26485024
10. Worasith C, Wongphutorn P, Homwong C, Kopolrat KY, Techasen A, Thanan R, et al. Effects of day-to-day variation of *Opisthorchis viverrini* antigen in urine on the accuracy of diagnosing opisthorchiasis in Northeast Thailand. *PLoS One*. 2022;17(7):e0271553. <https://doi.org/10.1371/journal.pone.0271553> PMID: 35853022
11. Worasith C, Sithithaworn J, Wongphutorn P, Homwong C, Khongsukwiwat K, Techasen A, et al. Accuracy of a new rapid diagnostic test for urinary antigen detection and assessment of drug treatment in opisthorchiasis. *Infect Dis Poverty*. 2023;12(1):102. <https://doi.org/10.1186/s40249-023-01162-4> PMID: 37990282
12. Subramanian I, Verma S, Kumar S, Jere A, Anamika K. Multi-omics data integration, interpretation, and its application. *Bioinform Biol Insights*. 2020;14:1177932219899051. <https://doi.org/10.1177/1177932219899051> PMID: 32076369
13. Hasin Y, Seldin M, Lusis A. Multi-omics approaches to disease. *Genome Biol*. 2017;18(1):83. <https://doi.org/10.1186/s13059-017-1215-1> PMID: 28476144
14. Khodadadian A, Darzi S, Haggi-Daredeh S, Sadat Eshaghi F, Babakhanzadeh E, Mirabutalebi SH, et al. Genomics and transcriptomics: the powerful technologies in precision medicine. *Int J Gen Med*. 2020;13:627–40. <https://doi.org/10.2147/IJGM.S249970> PMID: 32982380
15. Lowe R, Shirley N, Bleackley M, Dolan S, Shafee T. Transcriptomics technologies. *PLoS Comput Biol*. 2017;13(5):e1005457. <https://doi.org/10.1371/journal.pcbi.1005457> PMID: 28545146

16. Jex AR, Young ND, Sripa J, Hall RS, Scheerlinck J-P, Laha T, et al. Molecular changes in *Opisthorchis viverrini* (Southeast Asian liver fluke) during the transition from the juvenile to the adult stage. *PLoS Negl Trop Dis.* 2012;6(11):e1916. <https://doi.org/10.1371/journal.pntd.0001916> PMID: 23209858
17. Young ND, Nagarajan N, Lin SJ, Korhonen PK, Jex AR, Hall RS, et al. The *Opisthorchis viverrini* genome provides insights into life in the bile duct. *Nat Commun.* 2014;5:4378. <https://doi.org/10.1038/ncomms5378> PMID: 25007141
18. Chaidee A, Charoenram N, Sengthong C, Dangtakot R, Pinlaor P, Pongking T, et al. Transcriptome changes of liver fluke *Opisthorchis viverrini* in diabetic hamsters. *Parasite.* 2024;31:54. <https://doi.org/10.1051/parasite/2024056> PMID: 39269256
19. Geadkaew-Krenc A, Grams R, Siricoon S, Kosa N, Krenc D, Phadungsil W, et al. Cystatins from the human liver fluke *Opisthorchis viverrini*: molecular characterization and functional analysis. *Pathogens.* 2023;12(7):949. <https://doi.org/10.3390/pathogens12070949> PMID: 37513796
20. Salang R, Phadungsil W, Geadkaew-Krenc A, Grams R. Investigation of a serine protease inhibitor active in the infectious stage of the human liver fluke *Opisthorchis viverrini*. *Pathogens.* 2024;13(8):678. <https://doi.org/10.3390/pathogens13080678> PMID: 39204278
21. Pinlaor S, Onsurathum S, Boonmars T, Pinlaor P, Hongsrichan N, Chaidee A, et al. Distribution and abundance of *Opisthorchis viverrini* metacercariae in cyprinid fish in Northeastern Thailand. *Korean J Parasitol.* 2013;51(6):703–10. <https://doi.org/10.3347/kjp.2013.51.6.703> PMID: 24516277
22. Bhamarapravati N, Thammavit W, Vajrasthira S. Liver changes in hamsters infected with a liver fluke of man, *Opisthorchis viverrini*. *Am J Trop Med Hyg.* 1978;27(4):787–94. <https://doi.org/10.4269/ajtmh.1978.27.787> PMID: 686245
23. Jittimanee J, Sermswan RW, Puapairoj A, Maleewong W, Wongratanacheewin S. Cytokine expression in hamsters experimentally infected with *Opisthorchis viverrini*. *Parasite Immunol.* 2007;29(3):159–67. <https://doi.org/10.1111/j.1365-3024.2006.00929.x> PMID: 17266743
24. Andrews S. A quality control tool for high throughput sequence data. (Version v0.11.9) [Computer software]; 2010. Available from: <https://www.bioinformatics.babraham.ac.uk/projects/fastqc/>
25. Ewels P, Magnusson M, Lundin S, Käller M. MultiQC: summarize analysis results for multiple tools and samples in a single report. *Bioinformatics.* 2016;32(19):3047–8. <https://doi.org/10.1093/bioinformatics/btw354> PMID: 27312411
26. Kim D, Paggi JM, Park C, Bennett C, Salzberg SL. Graph-based genome alignment and genotyping with HISAT2 and HISAT-genotype. *Nat Biotechnol.* 2019;37(8):907–15. <https://doi.org/10.1038/s41587-019-0201-4> PMID: 31375807
27. Danecek P, Bonfield JK, Liddle J, Marshall J, Ohan V, Pollard MO, et al. Twelve years of SAMtools and BCFtools. *Gigascience.* 2021;10(2):giab008. <https://doi.org/10.1093/gigascience/giab008> PMID: 33590861
28. Anders S, Pyl PT, Huber W. HTSeq—a Python framework to work with high-throughput sequencing data. *Bioinformatics.* 2015;31(2):166–9. <https://doi.org/10.1093/bioinformatics/btu638> PMID: 25260700
29. R Core Team. R a language and environment for statistical computing: Reference index. R Foundation for Statistical Computing; 2010. Available from: <https://ringo.ams.stonybrook.edu/images/2/2b/Refman.pdf>
30. Love MI, Huber W, Anders S. Moderated estimation of fold change and dispersion for RNA-seq data with DESeq2. *Genome Biol.* 2014;15(12):550. <https://doi.org/10.1186/s13059-014-0550-8> PMID: 25516281
31. Wickham H. *ggplot2: Elegant graphics for data analysis.* 2nd ed. Springer International Publishing: Imprint: Springer; 2016. <https://doi.org/10.1007/978-3-319-24277-4>
32. Zhao S, Ye Z, Stanton R. Misuse of RPKM or TPM normalization when comparing across samples and sequencing protocols. *RNA.* 2020;26(8):903–9. <https://doi.org/10.1261/rna.074922.120> PMID: 32284352
33. Howe KL, Bolt BJ, Shafie M, Kersey P, Berriman M. WormBase ParaSite - a comprehensive resource for helminth genomics. *Mol Biochem Parasitol.* 2017;215:2–10. <https://doi.org/10.1016/j.molbiopara.2016.11.005> PMID: 27899279
34. Tao J, Hao Y, Li X, Yin H, Nie X, Zhang J, et al. Systematic identification of housekeeping genes possibly used as references in *caenorhabditis elegans* by large-scale data integration. *Cells.* 2020;9(3):786. <https://doi.org/10.3390/cells9030786> PMID: 32213971
35. Wang Z, Lyu Z, Pan L, Zeng G, Randhawa P. Defining housekeeping genes suitable for RNA-seq analysis of the human allograft kidney biopsy tissue. *BMC Med Genomics.* 2019;12(1):86. <https://doi.org/10.1186/s12920-019-0538-z> PMID: 31208411
36. Altschul SF, Gish W, Miller W, Myers EW, Lipman DJ. Basic local alignment search tool. *J Mol Biol.* 1990;215(3):403–10. [https://doi.org/10.1016/S0022-2836\(05\)80360-2](https://doi.org/10.1016/S0022-2836(05)80360-2) PMID: 2231712
37. Alexa A, Rahnenfuhrer J. *topGO: Enrichment analysis for gene ontology* (Version 2.50.0) [Computer software]; 2017. <https://doi.org/10.18129/B9.BIOC.TOPGO>
38. Protasio AV, Tsai IJ, Babbage A, Nichol S, Hunt M, Aslett MA, et al. A systematically improved high quality genome and transcriptome of the human blood fluke *Schistosoma mansoni*. *PLoS Negl Trop Dis.* 2012;6(1):e1455. <https://doi.org/10.1371/journal.pntd.0001455> PMID: 22253936
39. Wangwiwatsin A, Protasio AV, Wilson S, Owusu C, Holroyd NE, Sanders MJ, et al. Transcriptome of the parasitic flatworm *Schistosoma mansoni* during intra-mammalian development. *PLoS Negl Trop Dis.* 2020;14(5):e0007743. <https://doi.org/10.1371/journal.pntd.0007743> PMID: 32374726
40. Zhan Y, Qu Y, Zhu L, Shen C, Feng X, Yu C. Transcriptome analysis of tomato (*Solanum lycopersicum* L.) shoots reveals a crosstalk between auxin and strigolactone. *PLoS One.* 2018;13(7):e0201124. <https://doi.org/10.1371/journal.pone.0201124> PMID: 30044859
41. Brady CP, Dowd AJ, Brindley PJ, Ryan T, Day SR, Dalton JP. Recombinant expression and localization of *Schistosoma mansoni* cathepsin L1 support its role in the degradation of host hemoglobin. *Infect Immun.* 1999;67(1):368–74. <https://doi.org/10.1128/IAI.67.1.368-374.1999> PMID: 9864238

42. Caffrey CR, Goupil L, Rebello KM, Dalton JP, Smith D. Cysteine proteases as digestive enzymes in parasitic helminths. PLoS Negl Trop Dis. 2018;12(8):e0005840. <https://doi.org/10.1371/journal.pntd.0005840> PMID: 30138310
43. Cavallero S, Lombardo F, Su X, Salvemini M, Cantacessi C, D'Amelio S. Tissue-specific transcriptomes of *Anisakis simplex* (sensu stricto) and *Anisakis pegreffii* reveal potential molecular mechanisms involved in pathogenicity. Parasit Vectors. 2018;11(1):31. <https://doi.org/10.1186/s13071-017-2585-7> PMID: 29321072
44. Sajid M, McKerrow JH, Hansell E, Mathieu MA, Lucas KD, Hsieh I, et al. Functional expression and characterization of *Schistosoma mansoni* cathepsin B and its trans-activation by an endogenous asparaginyl endopeptidase. Mol Biochem Parasitol. 2003;131(1):65–75. [https://doi.org/10.1016/s0166-6851\(03\)00194-4](https://doi.org/10.1016/s0166-6851(03)00194-4) PMID: 12967713
45. Ayón-Núñez DA, Fragoso G, Bobes RJ, Laclette JP. Plasminogen-binding proteins as an evasion mechanism of the host's innate immunity in infectious diseases. Biosci Rep. 2018;38(5):BSR20180705. <https://doi.org/10.1042/BSR20180705> PMID: 30166455
46. González-Miguel J, Valero MA, Reguera-Gómez M, Mas-Bargues C, Bargues MD, Simón F, et al. Numerous *Fasciola* plasminogen-binding proteins may underlie blood-brain barrier leakage and explain neurological disorder complexity and heterogeneity in the acute and chronic phases of human fascioliasis. Parasitology. 2019;146(3):284–98. <https://doi.org/10.1017/S0031182018001464> PMID: 30246668
47. Ramajo-Hernández A, Pérez-Sánchez R, Ramajo-Martín V, Oleaga A. *Schistosoma bovis*: plasminogen binding in adults and the identification of plasminogen-binding proteins from the worm tegument. Exp Parasitol. 2007;115(1):83–91. <https://doi.org/10.1016/j.exppara.2006.07.003> PMID: 16962583
48. Egea L, Aguilera L, Giménez R, Sorolla MA, Aguilar J, Badía J, et al. Role of secreted glyceraldehyde-3-phosphate dehydrogenase in the infection mechanism of enterohemorrhagic and enteropathogenic *Escherichia coli*: interaction of the extracellular enzyme with human plasminogen and fibrinogen. Int J Biochem Cell Biol. 2007;39(6):1190–203. <https://doi.org/10.1016/j.biocel.2007.03.008> PMID: 17449317
49. Pirovich DB, Da'dara AA, Skelly PJ. *Schistosoma mansoni* glyceraldehyde-3-phosphate dehydrogenase enhances formation of the blood-clot lysis protein plasmin. Biol Open. 2020;9(3):bio050385. <https://doi.org/10.1242/bio.050385> PMID: 32098782
50. Cantacessi C, Hofmann A, Young ND, Broder U, Hall RS, Loukas A, et al. Insights into SCP/TAPS proteins of liver flukes based on large-scale bioinformatic analyses of sequence datasets. PLoS One. 2012;7(2):e31164. <https://doi.org/10.1371/journal.pone.0031164> PMID: 22384000
51. International Helminth Genomes Consortium. Comparative genomics of the major parasitic worms. Nat Genet. 2019;51(1):163–74. <https://doi.org/10.1038/s41588-018-0262-1> PMID: 30397333
52. Fernández R, Gabaldón T. Gene gain and loss across the Metazoa Tree of Life. 2020.
53. Knox C, Wilson M, Klinger CM, Franklin M, Oler E, Wilson A, et al. DrugBank 6.0: the DrugBank knowledgebase for 2024. Nucleic Acids Res. 2024;52(D1):D1265–75. <https://doi.org/10.1093/nar/gkad976> PMID: 37953279
54. Zheng Y, Young ND, Song J, Gasser RB. Genome-wide analysis of *haemonchus contortus* proteases and protease inhibitors using advanced informatics provides insights into parasite biology and host-parasite interactions. Int J Mol Sci. 2023;24(15):12320. <https://doi.org/10.3390/ijms241512320> PMID: 37569696
55. Nesterenko MA, Starunov VV, Shchenkov SV, Maslova AR, Denisova SA, Granovich AI, et al. Molecular signatures of the rediae, cercariae and adult stages in the complex life cycles of parasitic flatworms (Digenea: Psilostomatidae). Parasit Vectors. 2020;13(1):559. <https://doi.org/10.1186/s13071-020-04424-4>
56. Olson PD. Hox genes and the parasitic flatworms: new opportunities, challenges and lessons from the free-living. Parasitol Int. 2008;57(1):8–17. <https://doi.org/10.1016/j.parint.2007.09.007> PMID: 17977060
57. Cwiklinski K, Robinson MW, Donnelly S, Dalton JP. Complementary transcriptomic and proteomic analyses reveal the cellular and molecular processes that drive growth and development of *Fasciola hepatica* in the host liver. BMC Genomics. 2021;22(1):46. <https://doi.org/10.1186/s12864-020-07326-y> PMID: 33430759
58. Potter LR. Guanylyl cyclase structure, function and regulation. Cell Signal. 2011;23(12):1921–6. <https://doi.org/10.1016/j.cellsig.2011.09.001> PMID: 21914472
59. You Y, Kim J, Raizen DM, Avery L. Insulin, cGMP, and TGF-beta signals regulate food intake and quiescence in *C. elegans*: a model for satiety. Cell Metab. 2008;7(3):249–57. <https://doi.org/10.1016/j.cmet.2008.01.005> PMID: 18316030
60. Liu G-H, Korhonen PK, Young ND, Lu J, Wang T, Fu Y-T, et al. Dipylidium caninum draft genome - a new resource for comparative genomic and genetic explorations of flatworms. Genomics. 2021;113(3):1272–80. <https://doi.org/10.1016/j.ygeno.2021.02.019> PMID: 33677058
61. Zhang S. Comparative transcriptomic analysis of the larval and adult Stages of *Taenia pisiformis*. Genes (Basel). 2019;10(7):507. <https://doi.org/10.3390/genes10070507> PMID: 31277509
62. Anderson L, Amaral MS, Beckedorff F, Silva LF, Dazzani B, Oliveira KC, et al. *Schistosoma mansoni* egg, adult male and female comparative gene expression analysis and identification of novel genes by RNA-seq. PLoS Negl Trop Dis. 2015;9(12):e0004334. <https://doi.org/10.1371/journal.pntd.0004334> PMID: 26719891
63. Wang J, Chen R, Collins JJ 3rd. Systematically improved in vitro culture conditions reveal new insights into the reproductive biology of the human parasite *Schistosoma mansoni*. PLoS Biol. 2019;17(5):e3000254. <https://doi.org/10.1371/journal.pbio.3000254> PMID: 31067225
64. Cantacessi C, Gasser RB. SCP/TAPS proteins in helminths—where to from now? Mol Cell Probes. 2012;26(1):54–9. <https://doi.org/10.1016/j.mcp.2011.10.001> PMID: 22005034

65. Wong Y, Rosa BA, Becker L, Camberis M, LeGros G, Zhan B, et al. Proteomic characterization and comparison of the infective and adult life stage secretomes from *Necator americanus* and *Ancylostoma ceylanicum*. PLoS Negl Trop Dis. 2025;19(1):e0012780. <https://doi.org/10.1371/journal.pntd.0012780> PMID: 39832284
66. Leontovyc A, Ulrychová L, O'Donoghue AJ, Vondrášek J, Marešová L, Hubálek M, et al. SmSP2: a serine protease secreted by the blood fluke pathogen *Schistosoma mansoni* with anti-hemostatic properties. PLoS Negl Trop Dis. 2018;12(4):e0006446. <https://doi.org/10.1371/journal.pntd.0006446> PMID: 29677188
67. Jolly ER, Chin C-S, Miller S, Bahgat MM, Lim KC, DeRisi J, et al. Gene expression patterns during adaptation of a helminth parasite to different environmental niches. Genome Biol. 2007;8(4):R65. <https://doi.org/10.1186/gb-2007-8-4-r65> PMID: 17456242
68. Caña-Bozada VH, Huerta-Ocampo JA, Bojórquez-Velázquez E, Elizalde-Contreras JM, May ER, Morales-Serna FN. Proteomic analysis of *Neobenedenia* sp. and *Rhabdosynochus viridis* (Monogenea, Monopisthocotylea): insights into potential vaccine targets and diagnostic markers for finfish aquaculture. Vet Parasitol. 2024;329:110196. <https://doi.org/10.1016/j.vetpar.2024.110196> PMID: 38763120
69. Houhou H, Puckelwaldt O, Strube C, Haeberlein S. Reference gene analysis and its use for kinase expression profiling in *Fasciola hepatica*. Sci Rep. 2019;9(1):15867. <https://doi.org/10.1038/s41598-019-52416-x> PMID: 31676853
70. Pouchkina-Stantcheva NN, Cunningham LJ, Olson PD. Spatial and temporal consistency of putative reference genes for real-time PCR in a model tapeworm. Mol Biochem Parasitol. 2011;180(2):120–2. <https://doi.org/10.1016/j.molbiopara.2011.08.004> PMID: 21907248